Available online at www.sciencedirect.com
SCIENCE DIRECT®
ELSEVIER
International Journal of Solids and Structures 41 (2004) 6759–6782
INTERNATIONAL JOURNAL OF SOLIDS and STRUCTURES
www.elsevier.com/locate/ijsolstr

Deformation induced elasto-plastic anisotropy in metal foams – modelling and simulation

I. Schmidt *

Institut für Mechanik, Technische Universität Darmstadt, Hochschulstr. 1, D-64289 Darmstadt, Germany

Received 7 May 2004
Available online 15 July 2004

Abstract

This work tries to define, analyse and quantify the elastic and plastic anisotropy that develops after some deformation history involving finite (plastic) strains in a two dimensional cellular material. The internal variable framework for the description of elasto-plastic material behaviour in the presence of anisotropy is briefly reviewed; the multiplicative decomposition of the deformation gradient into elastic and plastic parts is utilised, which is viewed here as an inevitable consequence of the assumption of the existence of a range of elastic material response. It is shown that the stress thermodynamically conjugate to what is commonly called the plastic velocity gradient is symmetric, as a result of describing the elastic behaviour with – possibly evolving – structure tensors as additional arguments in the free energy function. Some existing formulations of anisotropic plasticity are compared, discussing in particular the formulations of the normality rule and the assumptions regarding the elastic behaviour. The main part of the article is devoted to the presentation of the simulated response, obtained by numerical homogenisation, of a two dimensional cellular model material to selected straining paths. Specifically, the evolving elastic and plastic anisotropies are characterised in terms of computed yield surfaces and surfaces of constant strain energy in stress space. It is found that the elastic and plastic anisotropies are closely related and do not differ significantly from an orthotropic symmetry whose axes coincide with the principal plastic stretch directions, even for strongly non-proportional loading paths.

Keywords: Plasticity; Anisotropy; Metallic foams; Homogenisation

1. Introduction

Advances in manufacturing technology during the past years have made metal foams available for industrial applications that exploit their specific mechanical, thermal and/or acoustic properties. Potential applications include, among others, energy absorbing components, sandwich structures and heat exchangers (Gibson and Ashby, 1998) and the successful utilisation of this type of material requires a thorough understanding of its mechanical properties. Due to their cellular microstructure, metal foams are capable of undergoing very large – usually compressive – strains. Because of the ductile behaviour of the cell wall

* Tel.: +49-6151-162974; fax: +49-6151-163018.
E-mail address: i.schmidt@mechanik.tu-darmstadt.de (I. Schmidt).

0020-7683/$ - see front matter © 2004 Elsevier Ltd. All rights reserved.
doi:10.1016/j.ijsolstr.2004.05.021

material, these large strains are accompanied by large irreversible changes in the geometry of the microstructure which, in turn, leads to significant changes in the (macroscopic) mechanical properties. In particular, an anisotropy in both elastic and plastic properties must be expected to evolve. This phenomenon was illustrated in Deshpande and Fleck (1999) where the uniaxial yield strength perpendicular to the direction of a prior uniaxial compression was determined experimentally and was found to be nearly twice that of the compressive direction. Other experiments show that the Young's modulus, measured by unloading a compressive specimen, is reduced to about half its initial value after 10% uniaxial logarithmic compressive strain (Bastawros et al., 2000). This type of behaviour is obviously not restricted to cellular materials: Fully dense, polycrystalline metals, e.g., develop a macroscopic anisotropy as a result chiefly of texture formation when they are 'heavily' deformed (Kocks et al., 1998). Usually, however, the changes in the elastic properties are relatively small and the texture evolution becomes important only for very large strains. In contrast, a high porosity of a material makes morphological changes of the microstructure easier and the effect of anisotropy evolution is much more pronounced. Another example in this context is the cold compaction of powders. Beginning from a dense random packed aggregate of the powder, the contact areas between individual particles grow and are created in response to a macroscopic stress. A non-hydrostatic macroscopic stress will induce an anisotropic distribution of these contact areas; at later stages of the process, when the material can be viewed as a solid containing voids, the shape of the voids will be non-spherical, again resulting in a macroscopic anisotropy (cf. Akisanya et al., 1985; Rottmann et al., 2001).

Even though the essentials of a theory for elasto-plastic material behaviour date back some decades (Hill, 1978; Mandel, 1974; Rice, 1971) there is an ongoing discussion about several aspects of fundamental nature. These relate to the identification of elastic and plastic strains and their rates, the appropriateness of certain invariance requirements, the role of whatever is meant by the term 'plastic spin' and also to the formulation of the normality law. The points of disagreement become particularly apparent when large elastic strains and/or anisotropy are considered. Some of the more recent publications in this context include (Miehe, 1998; Hackl, 1997; Svendsen, 2001; Dafalias, 1998; Scheidler and Wright, 2001; Rubin, 1994; Bertram, 1998).

Apart from the more fundamental differences, there is a multitude of specific yield criteria and hardening rules proposed in the literature that can hardly be overlooked. We mention the works of Papadopoulos and Lu (2001), Tsakmakis (2004), Bruhns et al. (1999), Reese (2003), Eidel and Gruttmann (2003), Menzel and Steinmann (2003), Ekh and Runesson (2001) and Sidoroff and Dogui (2001).

Often, the differences between the many proposals regarding both fundamental aspects and details of a specific model are hidden behind a large body of formulas and a comparison with other existing models is routinely not made. Since the primary purpose of this work is to analyse the evolving anisotropy in metallic foams, and since some concepts for its description are not generally agreed upon, it is necessary to spend some words on the aforementioned general aspects of the theory. In the course of doing so, some of the above mentioned models will be discussed; this is done in Section 2. Some definitions related to the homogenisation procedure are recalled in Section 3, followed by the presentation of the numerical results in Section 4.

2. Constitutive framework for elasto-plasticity

2.1. Internal variable formalism

Following Rice (1971) [1] or Coleman and Gurtin (1967), an internal variable description of rate independent inelastic material behaviour for an isothermal process is represented by constitutive relations for the Helmholtz free energy density ψ, per unit reference volume, and the Piola–Kirchhoff stress $\boldsymbol{P}$ in the form

[1] Rice's analysis is based on the consideration of representative volume element of the material and the 'internal variables' are not macroscopically defined quantities as in (1) but their rates are meant to represent microstructural changes at various sites in that representative volume.

$$\begin{aligned}\psi &= \psi_1(\boldsymbol{F}, \vec{\xi}),\\ \boldsymbol{P} &= \boldsymbol{P}(\boldsymbol{F}, \vec{\xi}),\end{aligned} \tag{1}$$

in which $\vec{\xi}$ denotes a set of n internal variables ξ_α, $\alpha = 1, \ldots, n$, embodying the past history of the deformation gradient $\boldsymbol{F}$ at the point of interest. The above relations need to be completed by the specification of the evolution of the internal variables in the form

$$\dot{\vec{\xi}}_\alpha = \lambda g_{1\alpha}(\boldsymbol{F}, \vec{\xi}), \tag{2}$$

where the multiplier λ is a positive homogeneous function of degree one in $\dot{\boldsymbol{F}}$. With the definition of thermodynamic conjugates to the ξ's, the 'forces'

$$\vec{f} = -\partial_{\vec{\xi}}\psi_1(\boldsymbol{F}, \vec{\xi}), \tag{3}$$

and the assumption that, at any instant, the stresses are determined through the usual potential relation

$$\boldsymbol{P} = \partial_{\boldsymbol{F}}\psi_1(\boldsymbol{F}, \vec{\xi}), \tag{4}$$

the dissipation rate density δ, per unit reference volume, is given by

$$\delta \equiv \boldsymbol{P} \cdot \dot{\boldsymbol{F}} - \dot{\psi}_1 = \vec{f} \cdot \dot{\vec{\xi}}. \tag{5}$$

The second law is then expressed in the form of the Clausius–Duhem inequality as $\delta \geqslant 0$, where the underlying hypotheses is that the process can be treated as a sequence of constrained equilibrium states.

Material frame indifferent forms of the above constitutive relations, satisfying

$$\left.\begin{aligned}\psi_1(\boldsymbol{Q}\boldsymbol{F}, \vec{\xi}) &= \psi_1(\boldsymbol{F}, \vec{\xi})\\ \boldsymbol{P}(\boldsymbol{Q}\boldsymbol{F}, \vec{\xi}) &= \boldsymbol{Q}\boldsymbol{P}(\boldsymbol{F}, \vec{\xi})\end{aligned}\right\} \quad \forall \boldsymbol{Q} : \boldsymbol{Q}^{\mathrm{T}} = \boldsymbol{Q}^{-1}, \tag{6}$$

read, as usual,

$$\begin{aligned}\psi &= \psi_2(\boldsymbol{E}, \vec{\xi}),\\ \boldsymbol{S} &= \partial_{\boldsymbol{E}}\psi_2(\boldsymbol{E}, \vec{\xi}),\\ \dot{\vec{\xi}}_\alpha &= \lambda g_{2\alpha}(\boldsymbol{E}, \vec{\xi})\end{aligned} \tag{7}$$

in terms of rotation invariant, conjugate stress and strain measures, e.g. the Green–Lagrange strain

$$\boldsymbol{E} = \frac{1}{2}(\boldsymbol{C} - \boldsymbol{1}), \quad \boldsymbol{C} = \boldsymbol{F}^{\mathrm{T}}\boldsymbol{F} \tag{8}$$

and the symmetric Piola–Kirchhoff stress

$$\boldsymbol{S} = \boldsymbol{F}^{-1}\boldsymbol{P}. \tag{9}$$

Finally, the yield function Ω of the material is introduced with $\Omega(\boldsymbol{S}) \leqslant 0$ specifying the domain, in stress space, of elastic material response.

In the following, the focus will be on 'associative' inelasticity and different versions of what is called 'normality rule' will be juxtaposed. In particular, the notion of normality in the sense of Rice (1971) and Hill and Rice (1973), as expressed through [2]

$$(\dot{\boldsymbol{E}})_{\mathrm{p}} \equiv \dot{\boldsymbol{E}} - \mathbb{C}^{-1}\dot{\boldsymbol{S}} = \lambda\partial_{\boldsymbol{S}}\Omega, \quad \text{where } \mathbb{C} = \partial^2_{\boldsymbol{E}\boldsymbol{E}}\psi_2(\boldsymbol{E}, \vec{\xi}), \tag{10}$$

[2] In (10) $(\dot{\boldsymbol{E}})_{\mathrm{p}}$ is not the time derivative of any tensorial quantity; in particular, it is not, in general, the time derivative of a 'plastic strain', however defined: the statement is independent of whether or not there exists a permanent strain after unloading.

and the so called standard dissipative medium flow rule, given by

$$\overrightarrow{\xi} = \lambda \partial_{\vec{f}} \Phi(\vec{f}, \vec{\xi}) \tag{11}$$

in terms of a flow potential Φ, will be considered. The statement (10), which holds for any work conjugate pair of stress and strain measure, any choice of reference configuration and unrestricted deformations, can be viewed as a consequence of assuming that the rate of each internal variable is governed by its associated thermodynamic force, i.e. $g_{2\alpha}(\boldsymbol{E}, \vec{\xi}) = h_\alpha(f_\alpha(\boldsymbol{E}, \vec{\xi}), \vec{\xi})$. While this is expressed here in terms of the macroscopic internal variables, it is emphasised that the underlying assumption in Rice (1971) leading to (10) is less restrictive: Neither ψ nor h_α needs to be a point function of the ξ's, only the dissipation is required to be expressible as in (5). On the other hand, the flow rule (11) can be seen as a consequence of the assumption that (i) the yield function is stress state dependent only through the thermodynamic forces $\vec{f}$, i.e.

$$\Omega(\boldsymbol{S}) = \Phi(\vec{f}(\boldsymbol{S}), \vec{\xi}), \tag{12}$$

and that (ii) the evolution of the internal variables takes place such that for a given stress state the dissipation (5) is maximised. This concept can be found, in different forms, in the works of Ziegler and Wehrli (1987), Halphen and Nguyen (1975) and Hill (1948).

Relation (10) is, in principle, experimentally verifiable because all quantities appearing there are measurable. Furthermore, it is implied by (11) which can therefore be excluded if (10) does not hold. Conversely, if (10) holds, then (11) represents a possible approach but the flow potential Φ appearing there is not measurable when the dimension of $\vec{f}$ is larger than that of $\boldsymbol{S}$.

2.2. Multiplicative split of the deformation gradient

Rather than beginning a further specification of the constitutive relations (1) and (2) with introducing the multiplicative decomposition of the deformation gradient (14) we prefer the following line of thought: The assumption that after some deformation history there always exists a range of elastic material response means that we can always use the elasticity relation (4) to define

$$\boldsymbol{F}_\mathrm{p} = \arg\min_{\boldsymbol{F}} [\psi_1(\boldsymbol{F}, \vec{\xi})]_{\vec{\xi}=\text{const.}} \Rightarrow \partial_{\boldsymbol{F}} \psi_1(\boldsymbol{F}, \vec{\xi})\Big|_{\boldsymbol{F}=\boldsymbol{F}_\mathrm{p}} = \boldsymbol{0} \tag{13}$$

which, of course, identifies the stress free intermediate configuration. As a consequence of (6), the definition (13) leaves unspecified the orthogonal part $\boldsymbol{R}_\mathrm{p}$, but uniquely determines the right stretch part $\boldsymbol{U}_\mathrm{p}$, of the polar decomposition $\boldsymbol{F}_\mathrm{p} = \boldsymbol{R}_\mathrm{p}\boldsymbol{U}_\mathrm{p}$. If we decide to take the configuration $\boldsymbol{F} = \boldsymbol{F}_\mathrm{p}$ with some arbitrarily chosen $\boldsymbol{R}_\mathrm{p}$ as the reference configuration then

$$\boldsymbol{F}_\mathrm{e} = \boldsymbol{F}\boldsymbol{F}_\mathrm{p}^{-1} = \boldsymbol{F}\boldsymbol{U}_\mathrm{p}^{-1}\boldsymbol{R}_\mathrm{p}^\mathrm{T} \tag{14}$$

is the deformation gradient based on that configuration. Suppose now that an experimentalist were given a plastically deformed piece of material whose elastic properties are to be determined, and suppose further that he or she is able to provide a functional relation

$$\widetilde{\boldsymbol{P}} = \widetilde{\boldsymbol{P}}(\boldsymbol{F}_\mathrm{e}) \tag{15}$$

for the Piola–Kirchhoff Stress $\widetilde{\boldsymbol{P}}$, based on the intermediate configuration, that accurately describes the elastic behaviour of the material. The free energy $\tilde{\psi}$, per unit volume of the intermediate configuration, of the material is then *necessarily* of the form (cf. Rice, 1975)

$$\tilde{\psi} = \tilde{\psi}_{1\mathrm{e}}(\boldsymbol{F}_\mathrm{e}) + \tilde{\psi}_\mathrm{p}, \tag{16}$$

where $\tilde{\psi}_{\mathrm{p}}$, an integration constant, is independent of $\boldsymbol{F}_{\mathrm{e}}$ and $\tilde{\psi}_{\mathrm{e1}}$ has the property

$$\widetilde{\boldsymbol{P}} = \partial_{\boldsymbol{F}_{\mathrm{e}}} \tilde{\psi}_{1\mathrm{e}}(\boldsymbol{F}_{\mathrm{e}}). \tag{17}$$

Material frame indifferent forms of (16) and (17) are given by

$$\begin{aligned} \tilde{\psi} &= \tilde{\psi}_{2\mathrm{e}}(\widetilde{\boldsymbol{E}}_{\mathrm{e}}) + \tilde{\psi}_{\mathrm{p}}, \\ \widetilde{\boldsymbol{S}} &= \partial_{\widetilde{\boldsymbol{E}}_{\mathrm{e}}} \tilde{\psi}_{2\mathrm{e}}(\widetilde{\boldsymbol{E}}_{\mathrm{e}}), \end{aligned} \tag{18}$$

in terms of the Green–Lagrange strain

$$\widetilde{\boldsymbol{E}}_{\mathrm{e}} = \frac{1}{2}(\widetilde{\boldsymbol{C}}_{\mathrm{e}} - \mathbf{1}), \quad \widetilde{\boldsymbol{C}}_{\mathrm{e}} = \boldsymbol{F}_{\mathrm{e}}^{\mathrm{T}} \boldsymbol{F}_{\mathrm{e}} \tag{19}$$

and the symmetric Piola–Kirchhoff stress

$$\widetilde{\boldsymbol{S}} = \boldsymbol{F}_{\mathrm{e}}^{-1} \widetilde{\boldsymbol{P}} \tag{20}$$

both referring to the intermediate configuration. Without loss of generality we can choose $\tilde{\psi}_{2\mathrm{e}}(\mathbf{0}) = 0$ so that $\tilde{\psi}_{2\mathrm{e}}$ and $\tilde{\psi}_{\mathrm{p}}$ represent, respectively, the recoverable strain energy and the free energy 'locked' in the material after unloading, since $\widetilde{\boldsymbol{S}}(\widetilde{\boldsymbol{E}}_{\mathrm{e}} = \mathbf{0}) = \mathbf{0}$ by definition.

Now if (18) describes anisotropic elasticity, then the argument list in the strain energy function must contain, apart from $\widetilde{\boldsymbol{E}}_{\mathrm{e}}$, additional tensorial arguments, denoted by, say, $\widetilde{\boldsymbol{M}}_i$, $i = 1, 2, \ldots$, such that $\tilde{\psi}_{2\mathrm{e}}$ becomes an isotropic function of its arguments, i.e. [3]

$$\tilde{\psi}_{2\mathrm{e}}(\boldsymbol{Q} * \widetilde{\boldsymbol{E}}_{\mathrm{e}}; \boldsymbol{Q} * \widetilde{\boldsymbol{M}}_i) = \tilde{\psi}_{2\mathrm{e}}(\widetilde{\boldsymbol{E}}_{\mathrm{e}}; \widetilde{\boldsymbol{M}}_i) \quad \forall \boldsymbol{Q} : \boldsymbol{Q}^{\mathrm{T}} = \boldsymbol{Q}^{-1}, \tag{21}$$

or, equivalently, in terms of function $\tilde{\psi}_{1\mathrm{e}}$:

$$\tilde{\psi}_{1\mathrm{e}}(\boldsymbol{F}_{\mathrm{e}} \boldsymbol{Q}^{\mathrm{T}}; \boldsymbol{Q} * \widetilde{\boldsymbol{M}}_i) = \tilde{\psi}_{1\mathrm{e}}(\boldsymbol{F}_{\mathrm{e}}; \widetilde{\boldsymbol{M}}_i) \quad \forall \boldsymbol{Q} : \boldsymbol{Q}^{\mathrm{T}} = \boldsymbol{Q}^{-1}. \tag{22}$$

Here, the notation $\boldsymbol{Q} * \boldsymbol{A}$ is defined through

$$(\boldsymbol{Q} * \boldsymbol{A})_{i_1 i_2 \ldots i_n} = Q_{i_1 k_1} Q_{i_2 k_2} \ldots Q_{i_n k_n} A_{k_1 k_2 \ldots k_n} \tag{23}$$

for a tensor $\boldsymbol{A}$ of nth order. Eq. (21) can be understood quite simply as the requirement that $\tilde{\psi}_{2\mathrm{e}}$ be independent of the choice of coordinate system with respect to which the components of $\widetilde{\boldsymbol{E}}_{\mathrm{e}}$ are written out. Alternatively, it can be understood as the requirement that the strain energy be independent of the orientation of the reference configuration: Had we chosen another reference configuration $\boldsymbol{F}_{\mathrm{p}}^{*}$, differing from the first only through $\boldsymbol{F}_{\mathrm{p}}^{*} = \boldsymbol{Q}\boldsymbol{F}_{\mathrm{p}}$, (i.e. $\boldsymbol{U}_{\mathrm{p}}^{*} = \boldsymbol{U}_{\mathrm{p}}$) then the Green–Lagrange strain and the structure tensors would be [4]

$$\begin{aligned} \widetilde{\boldsymbol{E}}_{\mathrm{e}}^{*} &= \boldsymbol{Q} * \widetilde{\boldsymbol{E}}_{\mathrm{e}}, \\ \widetilde{\boldsymbol{M}}_i^{*} &= \boldsymbol{Q} * \widetilde{\boldsymbol{M}}_i, \end{aligned} \tag{24}$$

and it is seen from (21) that such a change leaves the strain energy unaltered (the same holds for the free energy (16) because the constant $\tilde{\psi}_{\mathrm{p}}$ is trivially invariant). [5] With (14) we can now write

$$\tilde{\psi}_{1\mathrm{e}} = \tilde{\psi}_{1\mathrm{e}}(\boldsymbol{F}\boldsymbol{F}_{\mathrm{p}}^{-1}; \widetilde{\boldsymbol{M}}_i), \tag{25}$$

[3] In order to avoid the introduction of too many symbols, $\tilde{\psi}_{2\mathrm{e}}$ has been used in both (18) and (21) although the functions there have a different number of arguments.

[4] This is a consequence of (19) and (14) and the fact that $\boldsymbol{Q}$ represents a *rigid body rotation*.

[5] This point of view is also expressed in, e.g., Svendsen (2001), Dafalias (1998) and Lubarda and Krajcinovic (1995).

where it is important to note that $\boldsymbol{F}_\mathrm{p}$ and the $\widetilde{\boldsymbol{M}}_i$'s are *not independent* as expressed in $(24)_2$. For this reason, one cannot perform a partial differentiation with respect to $\boldsymbol{F}_\mathrm{p}$ holding $\widetilde{\boldsymbol{M}}_i$ fixed. Using (24) to define the structure tensors in the unrotated configuration by

$$\widehat{\boldsymbol{M}}_i = \boldsymbol{R}_\mathrm{p}^\mathrm{T} * \widetilde{\boldsymbol{M}}_i, \tag{26}$$

and applying (22) with $\boldsymbol{Q} = \boldsymbol{R}_\mathrm{p}^\mathrm{T}$, (25) reads

$$\tilde{\psi}_\mathrm{1e} = \tilde{\psi}_\mathrm{1e}(\boldsymbol{F}\boldsymbol{U}_\mathrm{p}^{-1}; \widehat{\boldsymbol{M}}_i). \tag{27}$$

Since the volumes in the reference and intermediate configuration differ by a factor $J_\mathrm{p} = \det \boldsymbol{U}_\mathrm{p}$, so that $\psi = J_\mathrm{p}\tilde{\psi}$, we are lead to the following form of the referential free energy density

$$\psi_1(\boldsymbol{F}, \vec{\xi}) = \underbrace{J_\mathrm{p}\tilde{\psi}_\mathrm{1e}(\boldsymbol{F}\boldsymbol{U}_\mathrm{p}^{-1}; \widehat{\boldsymbol{M}}_i)}_{\psi_\mathrm{1e}(\boldsymbol{F}, \boldsymbol{U}_\mathrm{p}, \widehat{\boldsymbol{M}}_i)} + \underbrace{J_\mathrm{p}\tilde{\psi}_\mathrm{p}(\vec{\zeta})}_{\psi_\mathrm{p}(\boldsymbol{U}_\mathrm{p}, \vec{\zeta})} = \bar{\psi}_1(\boldsymbol{F}, \boldsymbol{U}_\mathrm{p}, \widehat{\boldsymbol{M}}_i, \vec{\zeta}) \tag{28}$$

in which one identifies $\boldsymbol{U}_\mathrm{p}$ and the $\widehat{\boldsymbol{M}}_i$'s as distinguished members of the vector $\vec{\xi}$, the remaining part of which is denoted by $\vec{\zeta}$. It should be noted that, though (28) might suggest otherwise, ψ_p does not necessarily depend on $\boldsymbol{U}_\mathrm{p}$ explicitly, either through J_p or otherwise. Any such dependence, however, is either through the invariants of $\boldsymbol{U}_\mathrm{p}$ or through additional structural tensors which also transform with (24).

To summarise: The single requirement that after any inelastic deformation history there exists an elastic potential necessitates, without any further assumption that is not generally agreed upon,

(i) the additive structure of the free energy consisting of a 'locked in' free energy and a recoverable strain energy part, whose form is entirely determined through the measurable elastic response and
(ii) the invariance of the free energy with respect to the orthogonal part of $\boldsymbol{F}_\mathrm{p}$.

The significance of (28) arises from the fact that, within this framework, the stresses are assumed to be given by the potential relation (4) also for inelastic processes.

2.3. Flow rules

2.3.1. The general case

A crucial point in setting up the evolution equations for the internal variables is the identification of the thermodynamically conjugate forces (3). For the above derived structure of the referential free energy, without further specifying the functional form of ψ_p, the dissipation (5) takes the form

$$\delta = -(\partial_{\boldsymbol{U}_\mathrm{p}}\psi_\mathrm{1e}) \cdot \dot{\boldsymbol{U}}_\mathrm{p} - (\partial_{\widehat{\boldsymbol{M}}_i}\psi_\mathrm{1e}) \cdot (\widehat{\boldsymbol{M}}_i)^{\cdot} - \dot{\psi}_\mathrm{p}. \tag{29}$$

The first term in (29) can be rearranged as

$$-(\partial_{\boldsymbol{U}_\mathrm{p}}\psi_\mathrm{1e}) \cdot \dot{\boldsymbol{U}}_\mathrm{p} = -\left(\partial_{\boldsymbol{U}_\mathrm{p}}(J_\mathrm{p}\tilde{\psi}_\mathrm{1e})\boldsymbol{U}_\mathrm{p}^\mathrm{T}\right) \cdot \left(\dot{\boldsymbol{U}}_\mathrm{p}\boldsymbol{U}_\mathrm{p}^{-1}\right) = -J_\mathrm{p}\widehat{\boldsymbol{\Sigma}} \cdot \left(\dot{\boldsymbol{U}}_\mathrm{p}\boldsymbol{U}_\mathrm{p}^{-1}\right), \tag{30}$$

where

$$\widehat{\boldsymbol{\Sigma}} = \tilde{\psi}_\mathrm{1e}\mathbf{1} - \widehat{\boldsymbol{C}}_\mathrm{e}\widehat{\boldsymbol{S}} \tag{31}$$

is Eshelby's energy momentum tensor based on the unrotated intermediate configuration with $\widehat{\boldsymbol{C}}_\mathrm{e}$ and $\widehat{\boldsymbol{S}}$ given by $(19)_2$ and (20) evaluated with $\boldsymbol{R}_\mathrm{p} = \mathbf{1}$. The second term in (31) is known as (the negative of) Mandel's stress which would be the only term had we assumed either plastic incompressibility $J_\mathrm{p} \equiv 1$ or a specific dependence of the structural tensors on J_p. The term (30) can also be expressed as (see Appendix A)

$$-J_{\mathrm{p}}\widehat{\boldsymbol{\Sigma}}\cdot\left(\dot{\boldsymbol{U}}_{\mathrm{p}}\boldsymbol{U}_{\mathrm{p}}^{-1}\right)=\widehat{\boldsymbol{\Lambda}}\cdot\widehat{\boldsymbol{D}}_{\mathrm{p}}, \tag{32}$$

where

$$\widehat{\boldsymbol{D}}_{\mathrm{p}}=\left(\dot{\boldsymbol{U}}_{\mathrm{p}}\boldsymbol{U}_{\mathrm{p}}^{-1}\right)_{\mathrm{sy}}, \tag{33}$$

and the Cartesian components of the stress measure $\widehat{\boldsymbol{\Lambda}}$ with respect to a coordinate system aligned with the principal directions of $\boldsymbol{U}_{\mathrm{p}}$ are given by

$$\widehat{\Lambda}_{ij}=-J_{\mathrm{p}}\left(\widehat{\Sigma}_{ij}^{\mathrm{sy}}+\widehat{\Sigma}_{ij}^{\mathrm{sk}}\frac{\lambda_i^p-\lambda_j^p}{\lambda_i^p+\lambda_j^p}\right) \tag{34}$$

in which $\widehat{\Sigma}_{ij}^{\mathrm{sy}}$ and $\widehat{\Sigma}_{ij}^{\mathrm{sk}}$ denote, respectively, the corresponding components of the symmetric and skew symmetric part of $\widehat{\boldsymbol{\Sigma}}$, and λ_i^p are the principal values of $\boldsymbol{U}_{\mathrm{p}}$. With the notation

$$-\partial_{\widehat{\boldsymbol{M}}_i}\psi_{1\mathrm{e}}=\widehat{\boldsymbol{G}}_i \tag{35}$$

the dissipation is now expressed as

$$\delta=\widehat{\boldsymbol{\Lambda}}\cdot\widehat{\boldsymbol{D}}_{\mathrm{p}}+\widehat{\boldsymbol{G}}_i\cdot(\widehat{\boldsymbol{M}}_i)^{\cdot}-\dot{\psi}_{\mathrm{p}}. \tag{36}$$

For a standard dissipative medium the evolution equations would be of the form

$$\begin{aligned}\widehat{\boldsymbol{D}}_{\mathrm{p}}&=\lambda\partial_{\widehat{\boldsymbol{\Lambda}}}\Phi(\widehat{\boldsymbol{\Lambda}},\widehat{\boldsymbol{G}}_i),\\ (\widehat{\boldsymbol{M}}_i)^{\cdot}&=\lambda\partial_{\widehat{\boldsymbol{G}}_i}\Phi(\widehat{\boldsymbol{\Lambda}},\widehat{\boldsymbol{G}}_i).\end{aligned} \tag{37}$$

Since the two thermodynamic 'forces' $\widehat{\boldsymbol{\Lambda}}$ and $\widehat{\boldsymbol{G}}_i$ result from the deformation dependent part $\psi_{1\mathrm{e}}$ of the free energy via (34) and (35), their value will depend on the current stress state. The forces conjugate to all other internal variables $\vec{\zeta}$ are, in contrast, independent of the current stress state, because ψ_{p} does not depend on $\boldsymbol{F}$. It follows that the relation between the (measurable) yield surface in stress space Ω and the flow potential Φ (cf. (12)) is of the form

$$\Omega(\boldsymbol{S})=\Phi(\widehat{\boldsymbol{\Lambda}}(\boldsymbol{S}),\widehat{\boldsymbol{G}}_i(\boldsymbol{S})), \tag{38}$$

where we have omitted the dependence of Φ on the forces conjugate to the ζ's, which describe the hardening of the material. It is important to note that while the function $\Omega(\boldsymbol{S})$ is, in principle, experimentally measurable, $\Phi(\widehat{\boldsymbol{\Lambda}},\widehat{\boldsymbol{G}}_i)$ is not, because it is impossible to vary one of its arguments while keeping the other fixed: The knowledge of the yield surface in stress space, however precise, contains no information about the flow potential other than what is expressed in (38).

For the most general case in which the elastic properties are allowed to evolve arbitrarily, the normality rule (10) can be rewritten in terms of quantities defined on the (unrotated) intermediate configuration as

$$\widehat{\boldsymbol{D}}_{\mathrm{p}}=\lambda\partial_{\widehat{\boldsymbol{\Lambda}}}\Omega(\widehat{\boldsymbol{\Lambda}})+\widehat{\mathbb{R}}\,\widehat{\mathscr{A}}_i(\widehat{\boldsymbol{M}}_i)^{\cdot}. \tag{39}$$

The 4th order tensor $\mathbb{R}$ and the (2 + order-of-$\widehat{\boldsymbol{M}}_i$)th order tensors $\widehat{\mathscr{A}}_i$ depend on the current stress state and the plastic stretch and are given in Appendix B. Eq. (39) is the precise statement of 'normality' in the sense of Hill and Rice in the context of the widely used multiplicative decomposition of $\boldsymbol{F}$. In the large elastic strain case, the knowledge of the measurable yield surface in stress space does *not* allow for the determination of direction of plastic flow, unless the evolution of the structure tensors is specified. It is emphasised that the differentiation in (39) involves the yield surface Ω (in the space of the stress measure $\widehat{\boldsymbol{\Lambda}}$), in contrast to $(37)_1$ involving that of the flow potential Φ.

Remark: The right hand side of Eq. (32) can be transformed yet further to give

$$\widehat{\boldsymbol{\Lambda}} \cdot \widehat{\boldsymbol{D}}_{\mathrm{p}} = (\boldsymbol{R}_{\mathrm{p}} * \widehat{\boldsymbol{\Lambda}}) \cdot (\boldsymbol{R}_{\mathrm{p}} * \widehat{\boldsymbol{D}}_{\mathrm{p}}) = \widetilde{\boldsymbol{\Lambda}} \cdot \widetilde{\boldsymbol{D}}_{\mathrm{p}}, \tag{40}$$

and since

$$\widetilde{\boldsymbol{D}}_{\mathrm{p}} = \boldsymbol{R}_{\mathrm{p}} * \widehat{\boldsymbol{D}}_{\mathrm{p}} = \boldsymbol{R}_{\mathrm{p}} * \left(\dot{\boldsymbol{U}}_{\mathrm{p}} \boldsymbol{U}_{\mathrm{p}}^{-1}\right)_{\mathrm{sy}} = \left(\dot{\boldsymbol{F}}_{\mathrm{p}} \boldsymbol{F}_{\mathrm{p}}^{-1}\right)_{\mathrm{sy}}, \tag{41}$$

(40) identifies the symmetric tensor $\widetilde{\boldsymbol{\Lambda}} = \boldsymbol{R}_{\mathrm{p}} * \widehat{\boldsymbol{\Lambda}}$ as the work conjugate to what is commonly called the 'plastic velocity gradient'.

It is a simple matter to rewrite (37) in terms of quantities defined in the rotated intermediate configuration. Using (26) and (41) and the convention $\tilde{(\,)} = \boldsymbol{R}_{\mathrm{p}} * \hat{(\,)}$ the result is [6]

$$\begin{aligned} &\widetilde{\boldsymbol{D}}_{\mathrm{p}} = \lambda \underset{\sim}{\partial}_{\boldsymbol{\Lambda}} \Phi(\widetilde{\boldsymbol{\Lambda}}, \widetilde{\boldsymbol{G}}_i), \\ &(\widetilde{\boldsymbol{M}}_i)^{\square} \equiv (\widetilde{\boldsymbol{M}}_i)^{\cdot} - \widetilde{\boldsymbol{\Omega}}_{\mathrm{p}} \widetilde{\boldsymbol{M}}_i - \widetilde{\boldsymbol{M}}_i \widetilde{\boldsymbol{\Omega}}_{\mathrm{p}}^{\mathrm{T}} = \lambda \underset{\sim}{\partial}_{\boldsymbol{G}_i} \Phi(\widetilde{\boldsymbol{\Lambda}}, \widetilde{\boldsymbol{G}}_i), \end{aligned} \tag{42}$$

where the spin $\widetilde{\boldsymbol{\Omega}}_{\mathrm{p}} = \dot{\boldsymbol{R}}_{\mathrm{p}} \boldsymbol{R}_{\mathrm{p}}^{\mathrm{T}}$ can be prescribed *arbitrarily*.

2.3.2. Unchanged elastic properties

In metal plasticity, it is typically observed that 'the elastic properties' of the material are unaffected by plastic deformation. In particular, this is so for elastically isotropic polycrystals when texture effects are negligible and for anisotropic single crystals deforming by crystallographic slip. The meaning of this statement is that if

$$\boldsymbol{P} = \boldsymbol{h}(\boldsymbol{F}) \tag{43}$$

was the elasticity relation before the occurrence of plastic deformation, then

$$\widetilde{\boldsymbol{P}} = \boldsymbol{h}(\boldsymbol{F}_{\mathrm{e}}) \tag{44}$$

with the same function $\boldsymbol{h}$ *and some properly chosen* $\boldsymbol{R}_{\mathrm{p}}$ is the elasticity relation after a plastic deformation $\boldsymbol{U}_{\mathrm{p}}$. This identifies the so called isoclinic intermediate configuration which is characterised by the fact that the structure tensors $\widetilde{\boldsymbol{M}}_i$ in this configuration remain constant throughout the deformation:

$$(\widetilde{\boldsymbol{M}}_i)^{\cdot} = \boldsymbol{0}. \tag{45}$$

It is only in this case that we can attach a constitutive meaning to the orthogonal part of $\boldsymbol{F}_{\mathrm{p}}$: because of (45), the $\widetilde{\boldsymbol{M}}_i$ in (25) are constant parameters and the referential free energy takes the form

$$\psi_1(\boldsymbol{F}, \vec{\xi}) = \underbrace{J_{\mathrm{p}} \tilde{\bar{\psi}}_{1\mathrm{e}}(\boldsymbol{F}\boldsymbol{F}_{\mathrm{p}}^{-1})}_{\psi_{1\mathrm{e}}(\boldsymbol{F}, \boldsymbol{F}_{\mathrm{p}})} + \underbrace{J_{\mathrm{p}} \tilde{\bar{\psi}}_{\mathrm{p}}(\vec{\zeta})}_{\psi_{\mathrm{p}}(\boldsymbol{F}_{\mathrm{p}}, \vec{\zeta})} = \bar{\bar{\psi}}_1(\boldsymbol{F}, \boldsymbol{F}_{\mathrm{p}}, \vec{\zeta}). \tag{46}$$

By definition, function $\bar{\bar{\psi}}_1(\boldsymbol{F}, \boldsymbol{F}_{\mathrm{p}}, \vec{\zeta})$ in (46) is *not* invariant with respect to the orthogonal part of $\boldsymbol{F}_{\mathrm{p}}$, and it does not make sense to require such an invariance.

The same calculation that lead to (36) now gives

$$\delta = -J_{\mathrm{p}} \widetilde{\boldsymbol{\Sigma}} \cdot \widetilde{\boldsymbol{L}}_{\mathrm{p}} - \dot{\psi}_{\mathrm{p}}, \tag{47}$$

identifying the (non-symmetric) Eshelby stress as the work conjugate to the 'plastic velocity gradient'

$$\widetilde{\boldsymbol{L}}_{\mathrm{p}} = \dot{\boldsymbol{F}}_{\mathrm{p}} \boldsymbol{F}_{\mathrm{p}}^{-1} = \boldsymbol{R}_{\mathrm{p}} * \left(\dot{\boldsymbol{U}}_{\mathrm{p}} \boldsymbol{U}_{\mathrm{p}}^{-1}\right) + \dot{\boldsymbol{R}}_{\mathrm{p}} \boldsymbol{R}_{\mathrm{p}}^{\mathrm{T}}. \tag{48}$$

[6] Written out here for the case that the $\widetilde{\boldsymbol{M}}_i$'s are 2nd order tensors. More generally one has $(\widetilde{\boldsymbol{M}}_i)^{\square} \equiv \boldsymbol{R}_{\mathrm{p}} * \left[\boldsymbol{R}_{\mathrm{p}}^{\mathrm{T}} * \widetilde{\boldsymbol{M}}_i\right]^{\cdot}$.

With the above identification, the 'flow rule' *for a standard dissipative medium* would now be of the form

$$\widetilde{\boldsymbol{L}}_{\mathrm{p}} = \lambda \partial_{(-J_{\mathrm{p}}\widetilde{\boldsymbol{\Sigma}})} \Phi(-J_{\mathrm{p}}\widetilde{\boldsymbol{\Sigma}}) \tag{49}$$

which is, although seemingly different, just a special case of (37): The evolution equations $(37)_2$ for the structural tensors $\widehat{\boldsymbol{M}}_i$ have been replaced here by one for the orientation $\boldsymbol{R}_{\mathrm{p}}$ which is hidden in the skew symmetric part of (49). It is important to realise that, as in (37), the differentiation in (49) involves the flow potential Φ which, although in this case depending on only one single tensorial stress measure, must not be confused with the measurable yield surface in stress space Ω. The relation between the two is, as before,

$$\Omega(\boldsymbol{S}) = \Phi(-J_{\mathrm{p}}\widetilde{\boldsymbol{\Sigma}}(\boldsymbol{S})) \tag{50}$$

and the Hill and Rice statement of 'normality' reads

$$\widehat{\boldsymbol{D}}_{\mathrm{p}} = \lambda \partial_{\widehat{\boldsymbol{\Lambda}}} \Omega(\widehat{\boldsymbol{\Lambda}}) - \widehat{\mathbb{R}}\widehat{\mathscr{A}}_i(\widehat{\boldsymbol{\Omega}}_{\mathrm{p}}\widehat{\boldsymbol{M}}_i + \widehat{\boldsymbol{M}}_i\widehat{\boldsymbol{\Omega}}_{\mathrm{p}}^{\mathrm{T}}) \quad \text{with } \widehat{\boldsymbol{\Omega}}_{\mathrm{p}} = \boldsymbol{R}_{\mathrm{p}}^{\mathrm{T}}\dot{\boldsymbol{R}}_{\mathrm{p}}. \tag{51}$$

2.3.3. Isotropic elasticity

For completeness, the case of unchanged *isotropic* elastic properties (in the intermediate configuration) is recorded here. Due to the coaxiality of $\widetilde{\boldsymbol{C}}_{\mathrm{e}}$ and $\widetilde{\boldsymbol{S}}$, the Eshelby stress is symmetric in this case, $\widetilde{\boldsymbol{\Sigma}} = \widetilde{\boldsymbol{\Sigma}}^{\mathrm{T}}$, and is, up to a scalar factor, identical to the previously introduced stress measure $\widehat{\boldsymbol{\Lambda}}$ (cf. (34)):

$$\widehat{\boldsymbol{\Lambda}} = -J_{\mathrm{p}}\widetilde{\boldsymbol{\Sigma}}. \tag{52}$$

The dissipation consequently reads

$$\delta = \widehat{\boldsymbol{\Lambda}} \cdot \widehat{\boldsymbol{D}}_{\mathrm{p}} - \dot{\psi}_{\mathrm{p}} \tag{53}$$

and the standard dissipative medium flow rule becomes

$$\widetilde{\boldsymbol{D}}_{\mathrm{p}} = \lambda \partial_{\widetilde{\boldsymbol{\Lambda}}} \Phi(\widetilde{\boldsymbol{\Lambda}}). \tag{54}$$

Since now $\widetilde{\boldsymbol{\Lambda}}$ is the only stress dependent thermodynamic force, the relation between Φ and Ω is

$$\Omega(\boldsymbol{S}) = \Phi(\widehat{\boldsymbol{\Lambda}}(\boldsymbol{S})) \tag{55}$$

which shows that flow potential and yield surface are in this case identical functions. The Hill and Rice statement of normality becomes

$$\widehat{\boldsymbol{D}}_{\mathrm{p}} = \lambda \partial_{\widehat{\boldsymbol{\Lambda}}} \Omega(\widehat{\boldsymbol{\Lambda}}) \tag{56}$$

and is seen to be *equivalent* to (54) – in contrast to the anisotropic case where (39) is only necessary for (37).

2.3.4. Small elastic strains

In practically important cases the elastic strains are small, i.e. $||\tilde{\boldsymbol{E}}_{\mathrm{e}}|| \ll 1$, and it suffices to take function $\tilde{\psi}_{2\mathrm{e}}$ in (21) as quadratic in its first argument:

$$\tilde{\psi}_{2\mathrm{e}}(\widehat{\boldsymbol{E}}_{\mathrm{e}}; \widehat{\mathbb{C}}) = \frac{1}{2}\widehat{\boldsymbol{E}}_{\mathrm{e}} \cdot (\widehat{\mathbb{C}}\widehat{\boldsymbol{E}}_{\mathrm{e}}) \tag{57}$$

so that the elasticity relation is simply

$$\widehat{\boldsymbol{S}} = \widehat{\mathbb{C}}\widehat{\boldsymbol{E}}_{\mathrm{e}}. \tag{58}$$

Note that (58) implies the relation

$$\boldsymbol{S} = \mathbb{C}_0(\boldsymbol{E} - \boldsymbol{E}_{\mathrm{p}}) \tag{59}$$

in terms of referential quantities, where

$$\mathbb{C}_0 = J_\mathrm{p} \boldsymbol{F}_\mathrm{p}^{-1} * \widehat{\mathbb{C}}. \tag{60}$$

Therefore, if $\widehat{\mathbb{C}}$ is constant during an inelastic process, then $\mathbb{C}_0$ is not and vice versa. A similar statement holds if an additive split of generalised Lagrangean strain measures is used as in Papadopoulos and Lu (2001), Miehe et al. (2002) and Löblein et al. (2003). In these formulations, the linear elastic stiffness in the intermediate configuration does not remain constant (cf. Schmidt, in press).

The elastic stiffness tensor $\widehat{\mathbb{C}}$ now plays the role of one of the structure tensors introduced previously (there being only one of 4th order in this case). The conjugate 'force' is given by

$$\widehat{\mathbb{E}} \equiv -\partial_{\widehat{\mathbb{C}}}(J_\mathrm{p}\tilde{\psi}_{2\mathrm{e}}) = -J_\mathrm{p}\frac{1}{2}\widehat{\boldsymbol{E}}_\mathrm{e} \otimes \widehat{\boldsymbol{E}}_\mathrm{e}. \tag{61}$$

The stress measure $\hat{\boldsymbol{\Lambda}}$ in (34) reduces to

$$\hat{\boldsymbol{\Lambda}} \approx J_\mathrm{p}\widehat{\boldsymbol{S}} \approx \bar{\boldsymbol{\tau}}, \tag{62}$$

the back rotated Kirchhoff stress, so that in this case the standard dissipative medium flow rules would be

$$\begin{aligned} \widehat{\boldsymbol{D}}_\mathrm{p} &= \lambda \partial_{\bar{\boldsymbol{\tau}}} \Phi(\bar{\boldsymbol{\tau}}, \widehat{\mathbb{E}}), \\ \widehat{\mathbb{C}}^{\cdot} &= \lambda \partial_{\widehat{\mathbb{E}}} \Phi(\bar{\boldsymbol{\tau}}, \widehat{\mathbb{E}}). \end{aligned} \tag{63}$$

Regarding the Hill and Rice normality, the second term in (39) can be shown to be negligible, if the overall change of $\widehat{\mathbb{C}}$ is or, otherwise, if the plastic strain accompanying a significant change of $\widehat{\mathbb{C}}$ is finite (i.e. large compared to the elastic strain). Thus, with (62), (39) reduces to

$$\widehat{\boldsymbol{D}}_\mathrm{p} = \lambda \partial_{\bar{\boldsymbol{\tau}}} \Omega(\bar{\boldsymbol{\tau}}), \tag{64}$$

and this is indistinguishable from $(63)_1$. For future reference, the complementary elastic potential, per unit reference volume, is introduced here as

$$\varphi_\mathrm{e}(\bar{\boldsymbol{\tau}}) = \frac{1}{2}\bar{\boldsymbol{\tau}} \cdot ((J_\mathrm{p}\widehat{\mathbb{C}})^{-1}\bar{\boldsymbol{\tau}}), \tag{65}$$

so that

$$\widehat{\boldsymbol{E}}_\mathrm{e} = \partial_{\bar{\boldsymbol{\tau}}}\varphi_\mathrm{e}(\bar{\boldsymbol{\tau}}). \tag{66}$$

2.4. Comparison with other formulations

The formulation developed so far is similar to the work of Svendsen (2001) who also considered evolving structure tensors as additional arguments in the free energy function. The quantity $\widetilde{\boldsymbol{\Lambda}}$ has also been introduced there and has been calculated for a specific form of the strain energy function; the general explicit formulas (34)/(A.5) appear to be new. Moreover, the case of associated evolution equations is not considered in detail in Svendsens work and the different normality rules are not discussed.

The above formulation is also equivalent to that outlined in Miehe (1998) when his 'plastic metric' is identified with $\boldsymbol{U}_\mathrm{p}$, and a particular dependence of the free energy on that quantity is *assumed a priori*. The relation to models working with a nine dimensional internal variable $\boldsymbol{F}_\mathrm{p}$, i.e. $\boldsymbol{R}_\mathrm{p} \neq \boldsymbol{1}$, and also to models using an additive split of a Lagrangean strain measure is not discussed in detail. Also, we remark that the split of the free energy into volumetric and isochoric contributions, proposed by Miehe (1998), is only possible for the case of isotropy or orthotropy with cubic symmetry: For any other material symmetry, the deviatoric stresses will depend on the volumetric strains and vice versa.

Eq. (50) clearly shows the interrelation between the normal to the yield surface, the direction of plastic flow and the spin $\widehat{\boldsymbol{\Omega}}_{\mathrm{p}}$ (for the special case of unchanged elastic properties). A different form of it, namely

$$(\widetilde{\boldsymbol{C}}_{\mathrm{e}}\widetilde{\boldsymbol{L}}_{\mathrm{p}})_{\mathrm{sy}} + 2\widehat{\mathbb{C}}^{-1}(\widetilde{\boldsymbol{L}}_{\mathrm{p}}\widetilde{\boldsymbol{S}})_{\mathrm{sy}} = \lambda\partial_{\widetilde{\boldsymbol{S}}}\Omega(\widetilde{\boldsymbol{S}}), \tag{67}$$

containing the same physical statement for the special case of plastic incompressibility, $J_{\mathrm{p}} \equiv 1$, has been derived in Lubliner (1986) pointing out in particular the lacking equivalence to (49), which is questioned for this reason. The viewpoint taken here is that there is a conceptual difference between functions Ω and Φ which is not appreciated in Lubliner's article. [7]

Eq. (67), and therefore (51), is *not* equivalent to the normality rule proposed by Maugin (1994), which reads

$$(\widetilde{\boldsymbol{C}}_{\mathrm{e}}\widetilde{\boldsymbol{L}}_{\mathrm{p}})_{\mathrm{sy}} = \lambda\partial_{\widetilde{\boldsymbol{S}}}\Omega(\widetilde{\boldsymbol{S}}). \tag{68}$$

It is motivated by the fact that the first term in (47) is also expressible as [8]

$$-J_{\mathrm{p}}\tilde{\boldsymbol{\Sigma}}\cdot\tilde{\boldsymbol{L}}_{\mathrm{p}} = (\widehat{\boldsymbol{C}}_{\mathrm{e}}\widehat{\boldsymbol{S}})\cdot\widetilde{\boldsymbol{L}}_{\mathrm{p}} = \widehat{\boldsymbol{S}}\cdot(\widehat{\boldsymbol{C}}_{\mathrm{e}}\widetilde{\boldsymbol{L}}_{\mathrm{p}})_{\mathrm{sy}}, \tag{69}$$

due to the symmetry of $\widehat{\boldsymbol{S}}$, and so identifies the latter as the 'force' conjugate to the 'flux' $(\widehat{\boldsymbol{C}}_{\mathrm{e}}\widetilde{\boldsymbol{L}}_{\mathrm{p}})_{\mathrm{sy}}$. The reason for this discrepancy is that this flux is no time derivative of any quantity; it appears conceptually flaw to maximise (69) by comparing its value for different $\widehat{\boldsymbol{S}}$ at fixed $(\hat{\boldsymbol{C}}_{\mathrm{e}}\widetilde{\boldsymbol{L}}_{\mathrm{p}})_{\mathrm{sy}}$ because $\widehat{\boldsymbol{C}}_{\mathrm{e}}$ and $\widehat{\boldsymbol{S}}$ are obviously not independent.

Lubarda and Krajcinovic (1995) give a detailed discussion of the constitutive framework for damage-elasto-plasticity, i.e. plasticity accompanied by changing elastic properties. They particularly consider the case specified by (57) (but without restricting the magnitude of $\|\boldsymbol{E}_{\mathrm{e}}\|$). Their approach is characterised by introducing a further decomposition of the inelastic part $(\dot{\boldsymbol{E}})_{\mathrm{p}}$ of the strain rate (cf. (10)) into damage and plastic parts defined by $(\dot{\boldsymbol{E}})_{\mathrm{d}} = (\mathbb{C}_0^{-1})^{\cdot}\boldsymbol{S}$ and $(\dot{\boldsymbol{E}})_{\mathrm{pl}} = \dot{\boldsymbol{E}}_{\mathrm{p}} = (\dot{\boldsymbol{U}}_{\mathrm{p}}\boldsymbol{U}_{\mathrm{p}})_{\mathrm{sy}}$ respectively. The existence of *two different* potentials for the total inelastic and the damage part of the strain rate is then postulated such that [9]

$$(\dot{\boldsymbol{E}})_{\mathrm{p}} \propto \partial_{\boldsymbol{S}}\Omega(\boldsymbol{S}), \quad (\dot{\boldsymbol{E}})_{\mathrm{d}} \propto \partial_{\boldsymbol{S}}\Psi(\boldsymbol{S}). \tag{70}$$

In the associated case to be compared with the present approach, these potentials are identical to inelastic yield and damage functions, with the surfaces $\Omega = 0$ and $\Psi = 0$ identifying the boundary of the elastic domain and the onset of damage respectively. We remark that, since damage is clearly an inelastic process, Ω cannot be greater than Ψ. On the other hand, if damage occurs then both Ω and Ψ must be zero and since the two surfaces cannot intersect, they must share the same normal in stress space. This places severe restrictions on the functional forms of these potentials which seem difficult to satisfy in a specific model.

3. Homogenisation

The aim of the following sections is to determine, for a model material to be described shortly, the evolution of the elastic stiffness and the shape of the yield function, as defined in (57) and (64), for selected deformation histories. Specifically, the elastic and plastic anisotropies will be represented by iso-surfaces of

[7] The recent article of Cleja-Ţigoiu (2003) is also centred around the different normality statements but has not been fully understood by the present author.

[8] Plastic incompressibility is assumed here.

[9] More precisely, function Ψ is assumed to depend on the stress through $\boldsymbol{E} - \boldsymbol{E}_{\mathrm{p}}$, the referential counterpart of $\widehat{\mathbb{E}}$ in (61), and, in contrast to the yield function in the present article, function Ω is taken to depend also explicitly on the referential compliance $\mathbb{C}_0^{-1}$.

the yield function Ω and the strain energy φ in the space of the back rotated Kirchhoff stress $\bar{\boldsymbol{\tau}}$. These will be computed by a 'direct numerical homogenisation' considering a representative elementary volume (RVE) of a 2D cellular material. The details are briefly described next.

3.1. Macroscopic variables

Let $\mathscr{Z}$ denote the referential domain of the RVE, $\partial\mathscr{Z}$ its boundary with unit outward normal $\boldsymbol{N}$, V its volume, $\boldsymbol{x}$ the deformed position of a point originally located at $\boldsymbol{X}$ and $\boldsymbol{t}$ the traction vector. The macroscopic deformation gradient and Piola–Kirchhoff stress are defined as

$$\boldsymbol{F} = \frac{1}{V}\int_{\partial\mathscr{Z}} \boldsymbol{x}\otimes\boldsymbol{N}\,\mathrm{d}A, \quad \boldsymbol{P} = \frac{1}{V}\int_{\partial\mathscr{Z}} \boldsymbol{t}\otimes\boldsymbol{X}\,\mathrm{d}A \tag{71}$$

and from these other stress and strain measures are computed in the usual way. A rectangular two dimensional domain $\mathscr{Z}$ is considered and with $(\,)^{\pm}$ identifying cell edges opposite to each other, periodic boundary conditions on $\partial\mathscr{Z}$ are applied according to

$$\boldsymbol{x}^{+} - \boldsymbol{x}^{-} = \boldsymbol{F}(\boldsymbol{X}^{+} - \boldsymbol{X}^{-}), \quad \boldsymbol{t}^{+} + \boldsymbol{t}^{-} = \boldsymbol{0}. \tag{72}$$

3.2. Microstructure

As a 2D cellular model material an irregular hexagonal honeycomb structure as shown in Fig. 2(a) is considered. The structure is generated by randomly perturbing the vertex positions of a regular honeycomb up to 50% of the average cell wall length. With their length being large compared to the thickness, the cell walls are treated as slender beams. Moreover, one or two parabola-shaped wiggles are introduced in each beam as another typical imperfection observed in real metallic foams. The positions of vertices belonging to beams that cross the cell boundary are adjusted so as to produce a perfectly periodic structure without kinked beams. In terms of the beams' translational and rotational degrees of freedom $\boldsymbol{u}$ and $\boldsymbol{\phi}$ and their conjugates $\boldsymbol{f}$ and $\boldsymbol{m}$ the periodic boundary conditions are

$$\begin{aligned} &\boldsymbol{u}^{+} - \boldsymbol{u}^{-} = \nabla\mathbf{u}(\boldsymbol{X}^{+} - \boldsymbol{X}^{-}), && \boldsymbol{f}^{+} + \boldsymbol{f}^{-} = \boldsymbol{0}, \\ &\boldsymbol{\phi}^{+} - \boldsymbol{\phi}^{-} = \boldsymbol{0}, && \boldsymbol{m}^{+} + \boldsymbol{m}^{-} = \boldsymbol{0} \end{aligned} \tag{73}$$

with $\nabla\mathbf{u}$ denoting the macroscopic displacement gradient. This allows to prescribe separately histories for each single component of either the macrodisplacement gradient or the macro-Piola–Kirchhoff stress on a Cartesian basis coinciding with the normals to the cell faces.

The cell wall material is taken to be elastic-ideally plastic with Young's modulus $E = 5\times10^{4}$ N/mm^2 and yield strain $\epsilon_{\mathrm{y}} = 0.2\%$. The ratio of thickness to average beam length is $t/\ell = 0.05$ and the height of the wiggles is up to 0.07ℓ. No hardening, neither isotropic nor kinematic, is assumed on the microlevel in order to bring about the influence of the changing geometry of the microstructure. The RVE is approximately of square shape with edge length $\approx$14 cells. The beams are discretised with up to seven linear Timoshenko beam elements and the numerical computation has been performed using the commercial FEM code ABAQUS/explicit.

3.3. Elastic and plastic properties

At selected points in a loading programme, the deformation process is interrupted and the linear response at frozen inelastic variables to three independent macroscopic strains is used to compute the (referential) elastic stiffness via numerical differentiation:

$$\mathbb{C} = \left.\frac{\partial \boldsymbol{S}}{\partial \boldsymbol{E}}\right|_{\boldsymbol{E}_\mathrm{p}=\mathrm{const.}}. \tag{74}$$

From this, the current plastic stretch is computed as

$$\boldsymbol{U}_\mathrm{p} = \sqrt{\boldsymbol{C} - 2\mathbb{C}^{-1}\boldsymbol{S}} \tag{75}$$

and the stiffness in the unrotated intermediate configuration follows as

$$\widehat{\mathbb{C}} = J_\mathrm{p}^{-1}\boldsymbol{U}_\mathrm{p} * \mathbb{C}. \tag{76}$$

Subsequently, the structure is unloaded to (approximately) zero macroscopic stress by prescribing a total deformation equal to the above determined plastic stretch. If the elastic stiffness computed from (74) were exact, this would obviously correspond to $\boldsymbol{S} = \boldsymbol{0}$ exactly. Hence, the deviation of $\boldsymbol{S}$ from zero after this unloading is a measure for the quality of both the assumption of linear elastic response and the way to compute $\mathbb{C}$ and $\boldsymbol{U}_\mathrm{p}$.

To determine the yield surface, the RVE is then loaded in a prescribed stress space direction until the deviation from linearity – as defined by the previously computed stiffness and plastic strain – is greater than a certain offset. In particular,

$$\|(\boldsymbol{E} - \boldsymbol{E}_\mathrm{p}) - \mathbb{C}^{-1}\boldsymbol{S}\| > \epsilon \tag{77}$$

is taken to define yield, where ϵ is typically chosen as 0.2%. Moreover, the plastic part of the strain rate, as defined by the left hand side of (10), is evaluated for this particular loading direction. This procedure is repeated for different stress space directions until the yield surface is sufficiently well resolved.

The elastic and plastic properties so determined are depicted as plane sections through the yield surface and the surface of constant (complementary) strain energy in a three dimensional coordinate system with axes p, d and z, where

$$p = \frac{1}{2}\sqrt{2}(\bar{\tau}_{22} + \bar{\tau}_{11}), \quad d = \frac{1}{2}\sqrt{2}(\bar{\tau}_{22} - \bar{\tau}_{11}), \quad z = \sqrt{2}\bar{\tau}_{12} \tag{78}$$

in terms of the components of the back rotated Kirchhoff stress in a Cartesian basis coinciding with the normals to the cell faces. In this representation, an isotropic function of $\boldsymbol{\tau}$ is a surface of revolution around the p-axis; in particular, an isotropic quadratic function is an ellipsoid of revolution. An orthotropic function of $\boldsymbol{\tau}$ is less simple to recognise in the said plot; in order to quantify the deviation of the stiffness moduli $\widehat{\mathbb{C}}$ from orthotropy, a measure is introduced according to

$$\epsilon_\mathrm{ort} = \min_{\widehat{\mathbb{C}}_\mathrm{ort}} \frac{\|\widehat{\mathbb{C}} - \widehat{\mathbb{C}}_\mathrm{ort}\|}{\|\widehat{\mathbb{C}}\|} \tag{79}$$

which is the normalised distance from the 'closest' orthotropic stiffness tensor $\widehat{\mathbb{C}}_\mathrm{ort}$. If $\widehat{\mathbb{C}}$ has orthotropic symmetry, then $\epsilon_\mathrm{ort} = 0$, otherwise $\epsilon_\mathrm{ort} > 0$. Some details are given in Appendix C. The orientation of the orthotropy axes of that 'closest' orthotropic stiffness tensor is a byproduct of calculating ϵ_ort; this orientation is characterised by the angle φ_ort it encloses with the x_1 direction.

4. Results

4.1. Uniaxial compression

The first 'experiment' is a uniaxial compression in 2-direction where the lateral extension and a possible shear deformation is unconstrained. This is achieved through setting $P_{11} = P_{21} = \nabla u_{12} = 0$ and prescribing a non-zero value for ∇u_{22} (cf. Asaro and Needleman, 1985). Fig. 1 shows the stress response as plots of each component of $\boldsymbol{\tau}$ versus the corresponding component of the logarithmic stretch $\ln \boldsymbol{U}$. The compressive 22-stress shows the typical, known from experiments, extended 'plateau' regime after an initial linear segment (Miehe, 1998). [10] A sequence of the deformation patterns within the RVE is shown in Fig. 2. Above a compression of 15%, bands of highly deformed cells develop as is seen in the deformation picture fore stage (d). This, too, is observed in experimental investigations, cf. Bastawros et al. (2000). In the last stage (f), a second band of collapsing cells has formed and it is interesting to note that the spacing between the two bands is ≈4 cells which is precisely what is observed in a closed cell aluminum foam in the above mentioned article. Fig. 3 depicts the yield surface (solid line) and the surface of constant complementary strain energy (dashed line) at three different levels of compression: (a) 1%, (c) 10% and (f) 30% where the labels correspond to the stages shown in Fig. 2. These surfaces are represented by three sections with the coordinate planes in '*pdz* space'. Also shown is a trajectory of the stress path as a bold solid line. Since $\bar{\tau}_{11} = \bar{\tau}_{12} = 0$ it lies on the line $p = d$ in the p–d plane. Finally, the direction of the inelastic strain rate as computed from

$$\widehat{\boldsymbol{D}}_{\mathrm{p}} = \boldsymbol{U}_{\mathrm{p}}^{-\mathrm{T}}(\dot{\boldsymbol{E}})_{\mathrm{p}}\boldsymbol{U}_{\mathrm{p}}^{-1}, \tag{80}$$

valid for small elastic strains, is indicated with arrows along the yield surface. It can be seen that at all points these are indeed normal to the yield surface, as expected. Initially (Fig. 3(a)), the yield surface exhibits an asymmetry in that the hydrostatic strength is different in tension and compression ($d = z = 0$). But it is practically isotropic as can be concluded from the nearly circular shape in the d–z plane and the symmetry of its shape with respect to the p-axis. The same holds for the strain energy surface: by definition this is an ellipsoid and the plots show that it is an ellipsoid of revolution about the p-axis corresponding to an isotropic stiffness $\widehat{\mathbb{C}}$ (Fig. 3(a)). With ongoing deformation this ellipsoid gradually changes to have its major principal axes oriented approximately along the line $p = -d$ in stage (f), with little deviation from an ellipsoid of revolution. The same, in turn, can be said about the yield surface: regarding its overall appearance, it gradually changes to a convex surface with its major dimension oriented in that same direction. Note that this provides a picture, in terms of yield surface evolution, for the experimentally observed increase of the uniaxial yield strength perpendicular to the uniaxial compression direction (Deshpande and Fleck, 1999): In the p–d plane, uniaxial compression in the transverse direction corresponds to the line $p = -d > 0$ which is just the direction into which the major dimension of the yield surface is rotated. Thus the ratio of transverse to axial yield strength is expected to increase as experimentally observed.

The deviation of the yield surface from an ellipsoidal shape is firstly the mentioned asymmetry in hydrostatic tension and compression (at early and intermediate stages), and secondly a 'bulge' in the vicinity of the actual stress point. [11]

To further characterise the evolution of the stiffness, the three principal values of the 2D 4th order tensor $\widehat{\mathbb{C}}$, which correspond to the squares of the semiaxes of the strain energy ellipsoid, are plotted against the load parameter (in this case the uniaxial compression) in Fig. 4. The principal stiffness c_3, corresponding

[10] Because $J < 1$ in this case, the compressive stress would not decrease if the 22-component of the Cauchy stress where plotted instead of the Kirchhoff stress.

[11] This indicates a vertex formation at the current stress point as predicted on theoretical grounds (Hill, 1967); a detailed examination of this aspect will be presented in a forthcoming publication.

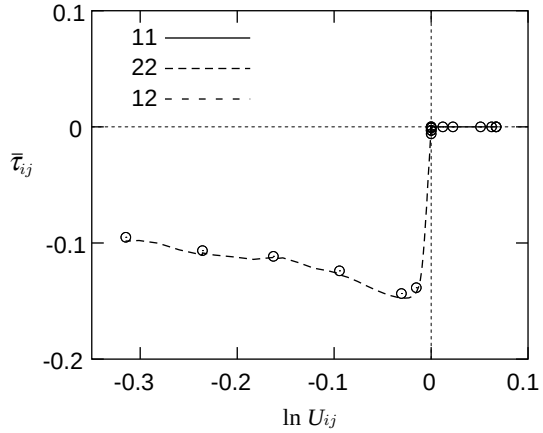

Fig. 1. Stress response to uniaxial compression. Each component of $\bar{\tau}$ is plotted versus the corresponding component of $\ln \boldsymbol{U}$.

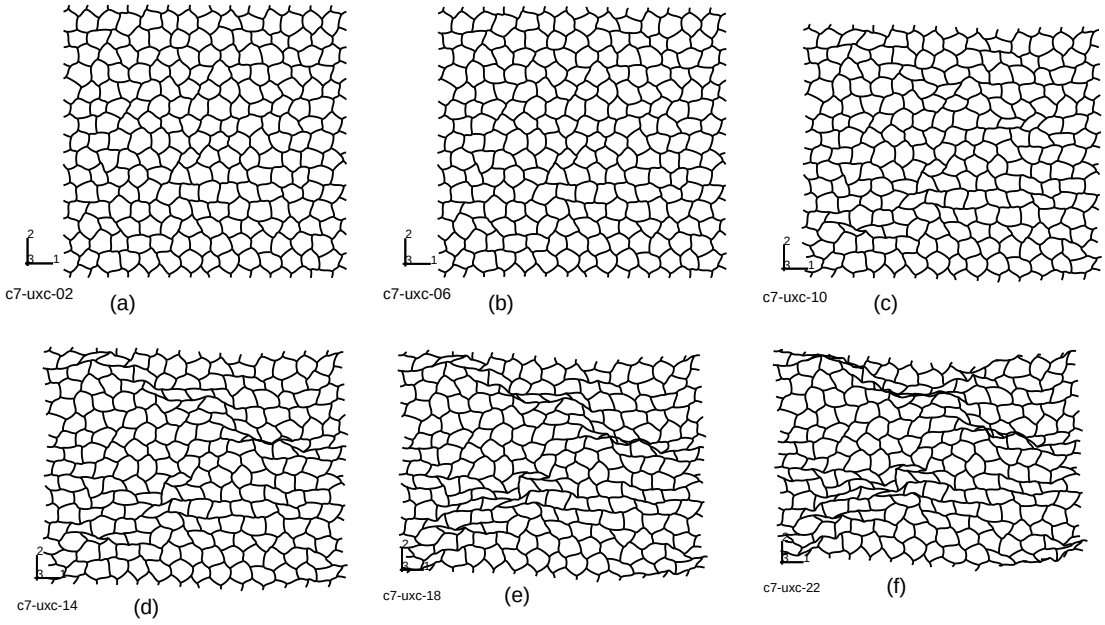

Fig. 2. Deformed configurations of the RVE at different load levels for uniaxial compression. The individual pictures correspond to the markers in Fig. 1.

initially to the compression modulus, is reduced to 40% of its initial value. Stiffness c_2, corresponding initially to a shear modulus, increases by 10% and then returns to its initial value, while c_1 remains essentially unchanged. The deviation from orthotropy as defined by (79) and the corresponding orientation of the 'closest' orthotropy axes and the principal plastic stretch are shown in Fig. 5. As could be expected

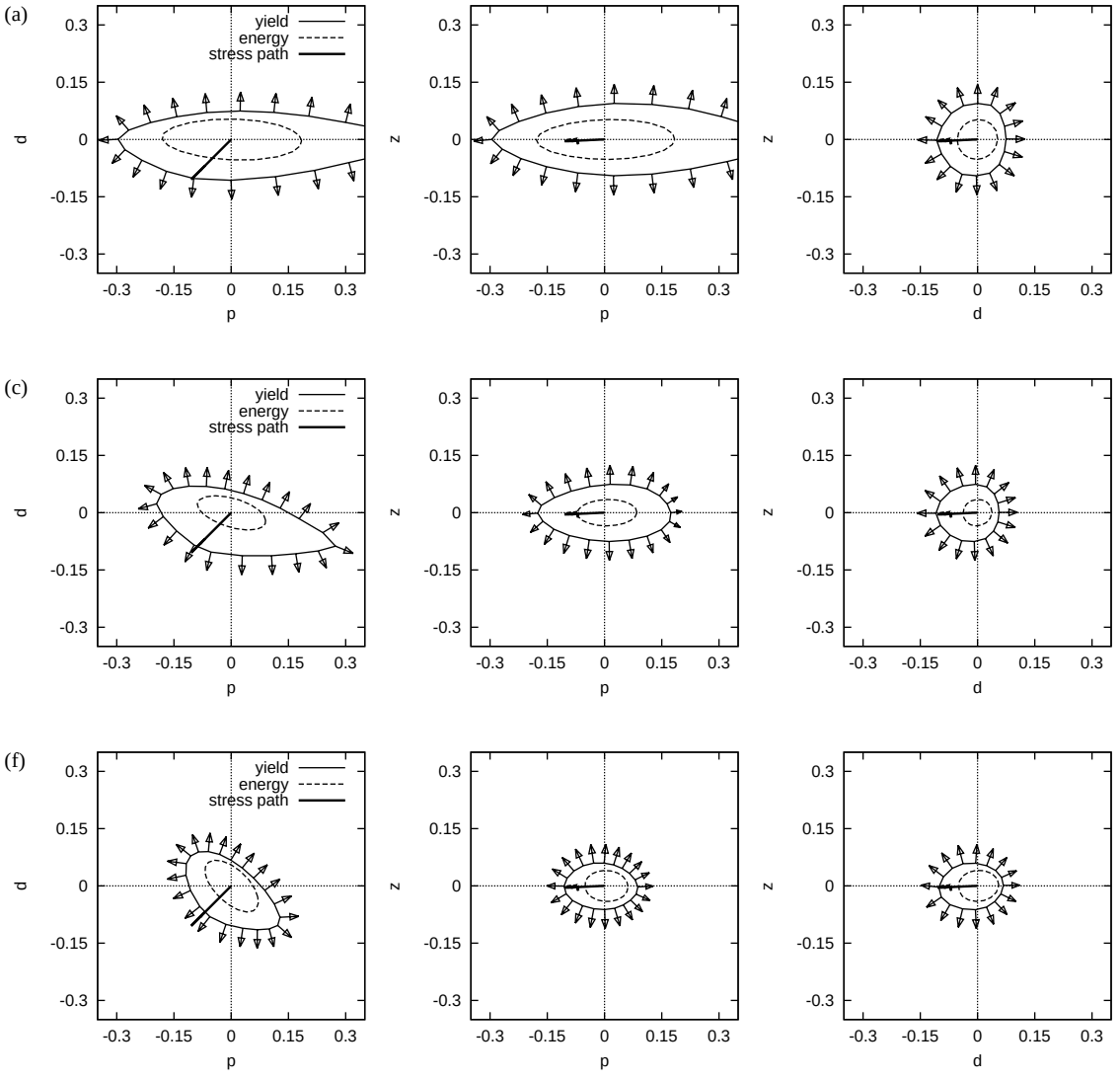

Fig. 3. Yield and energy surface and direction of inelastic strain rate in stress space after (a) 1%, (c) 10% and (f) 30% uniaxial compression.

for this proportional loading, the deviation from orthotropy is vanishingly small (Fig. 5(a)) and the corresponding orientation differs from zero – the plastic stretch direction – by only a few degrees (Fig. 5(b)). [12]

4.2. Hydrostatic compression

For a prescribed hydrostatic compression with $\nabla u_{11} = \nabla u_{22}$ and $\nabla u_{12} = P_{21} = 0$, the simulated stress response shown in Fig. 6 exhibits a significant drop in the compressive normal stresses after initial yield

[12] The first data point in the φ_{ort}-plot is actually meaningless because at this stage $\widehat{\mathbb{C}}$ is nearly isotropic and any small deviation from isotropy leads to finite values for φ_{ort}.

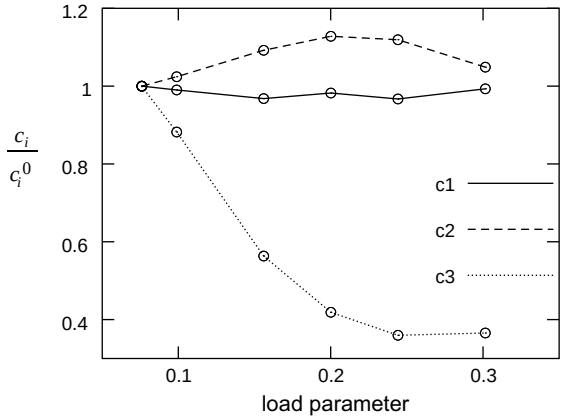

Fig. 4. Normalised principal stiffnesses versus load parameter for the uniaxial compression test.

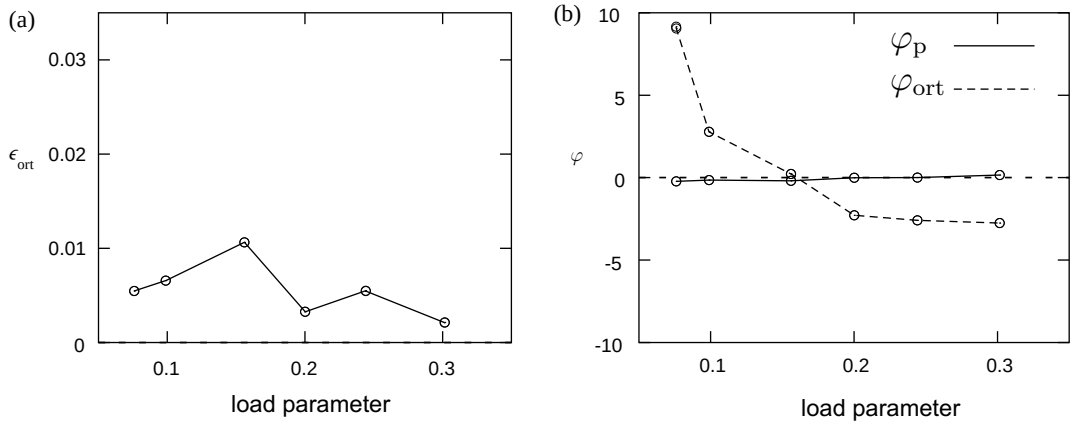

Fig. 5. Non-orthotropy measure ϵ_{ort} (a) and orientations φ_{ort} and φ_p of closest orthotropy direction and principal plastic stretch (b) for the uniaxial compression test.

with a subsequent plateau regime. As in the case of uniaxial compression, the compressive *Cauchy* stresses would actually increase in the final stage because J decreases exponentially with $\ln \boldsymbol{U}$. The sharp pressure drop, however, would remain and is in contrast to experimental observations. This effect is likely to be related to the fact that a two dimensional model is used here; first results using a three dimensional beam network do not exhibit this pressure drop but instead show a significant hardening.

Yield and energy surfaces after 25% hydrostatic compression are shown in Fig. 7. Isotropy in both is maintained and the yield surface assumes an egg-like shape, again with a bulge at the loading point. As before, the inelastic strain rate is found to be normal to the yield surface at all points.

4.3. Non-proportional loading

Both cases considered so far represent proportional loadings: The principal stretch directions remain fixed during deformation. Therefore the retained isotropy for hydrostatic compression and the developing

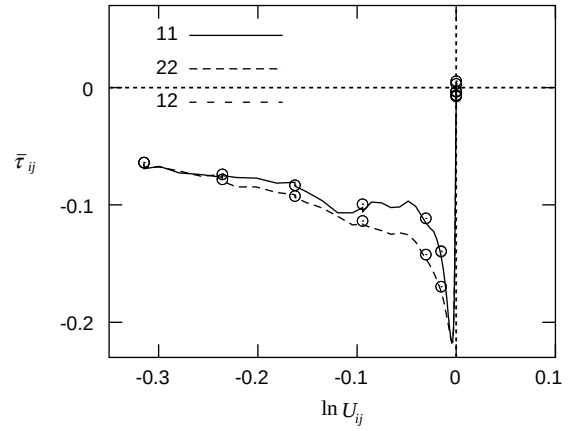

Fig. 6. Stress response to hydrostatic compression.

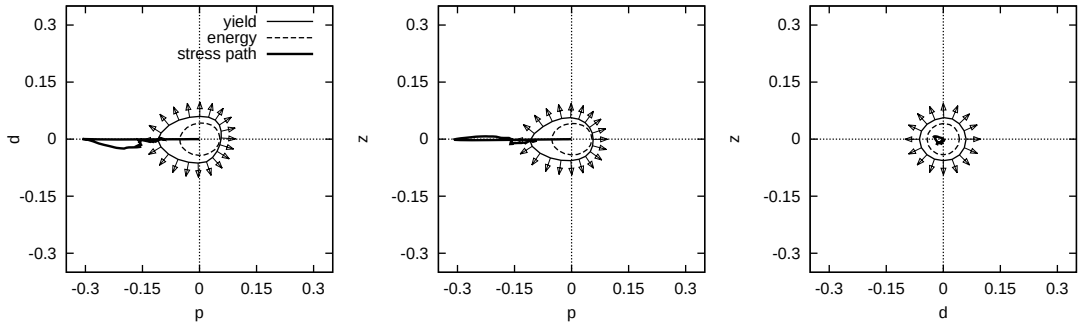

Fig. 7. Yield and energy surface and direction of inelastic strain rate in stress space after 25% hydrostatic compression.

orthotropy for uniaxial compression are not surprising. To examine the effect of non-proportional loading, a deformation history has been prescribed where the principal plastic stretches change monotonically to $\approx$1.1 and 0.8 respectively, while the principal stretch direction rotates from zero to $-35°$ relative to the x_1-axis. The corresponding snapshots of the deformed RVE are shown in Fig. 9. In stage (c), a band of collapsed cells has formed like in the uniaxial case. A closer inspection shows that the orientation of this band coincides with the principal stretch direction present at this stage – as could be expected. The stress response is depicted in Fig. 8; it is rather difficult to interpret since all stress components are non-zero. But it should be kept in mind that this somewhat unrealistic straining path is only meant to produce significant changes of principal stretch direction. Yield and energy surface corresponding to stage (e) in Fig. 9 are shown in Fig. 10. Like in the previous cases, the sections of yield and energy surfaces with the coordinate planes exhibit similar shapes – save for the bulge at the loading point in the yield surface. The deviation of the stiffness from orthotropy is visualised in Fig. 11(a) through the non-orthotropy measure ϵ_{ort}. Note that the relative distance from the closest orthotropic stiffness is just 2% in the final stage. In view of the finite stretches whose directions have swept over the material by a finite angle, this is a remarkable result. The orientation of this direction of orthotropy is found to approximately coincide, at all stages, with the changing direction of the principal plastic stretch – at least no other conclusion can be drawn from Fig. 11(b).

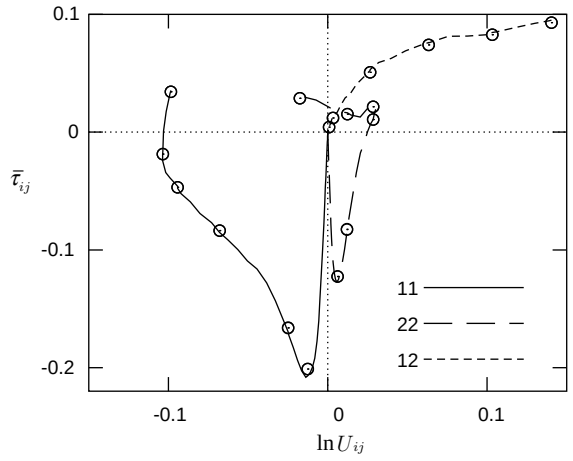

Fig. 8. Stress response to strongly non-proportional loading.

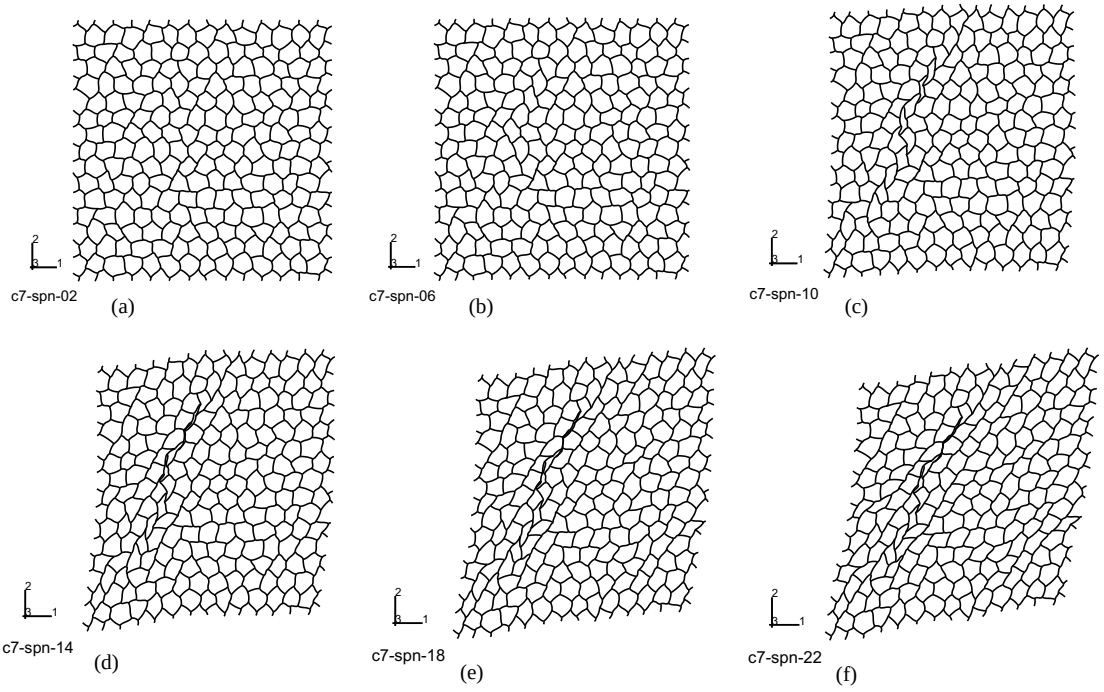

Fig. 9. Deformed configurations of the RVE at different load levels for strongly non-proportional loading. The individuals pictures correspond to the markers in Fig. 8.

Finally, the evolution of the principal stiffnesses is plotted in Fig. 12. It differs qualitatively from that for uniaxial compression (Fig. 4) – even though the final values of the stretch are similar: The principal stiffness labelled c_3, which corresponds to the initial compression modulus, first diminishes and then increases again

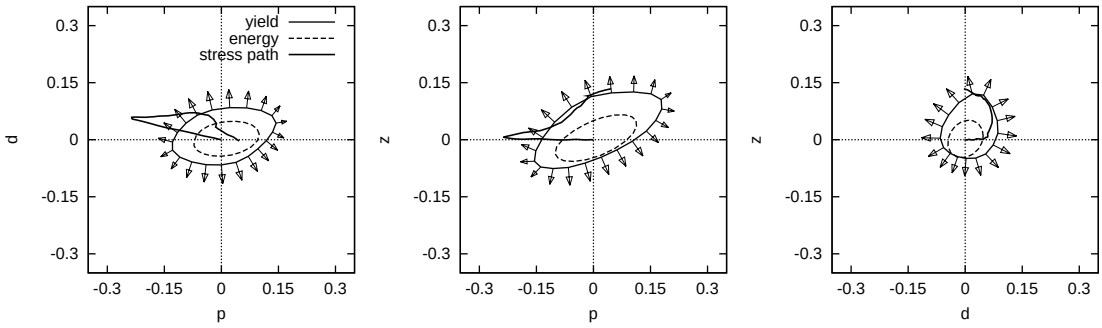

Fig. 10. Yield and energy surface and direction of inelastic strain rate in stress space after strongly non-proportional loading.

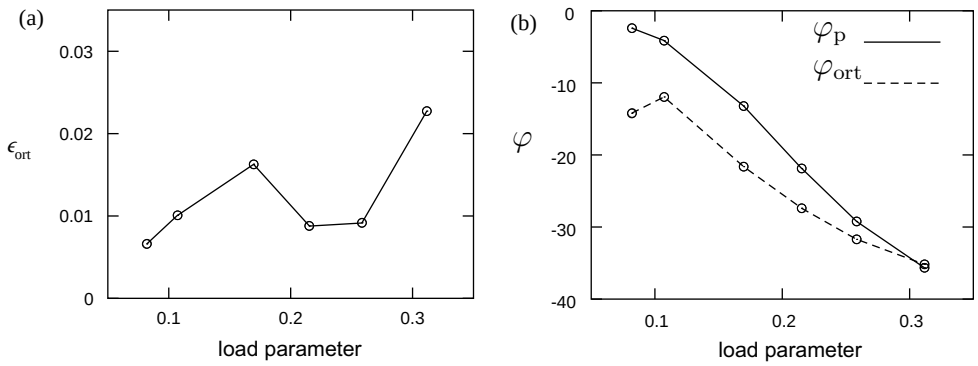

Fig. 11. Non-orthotropy measure ϵ_{ort} (a) and orientations φ_{ort} and φ_p of closest orthotropy direction and principal plastic stretch (b) for a strongly non-proportional loading.

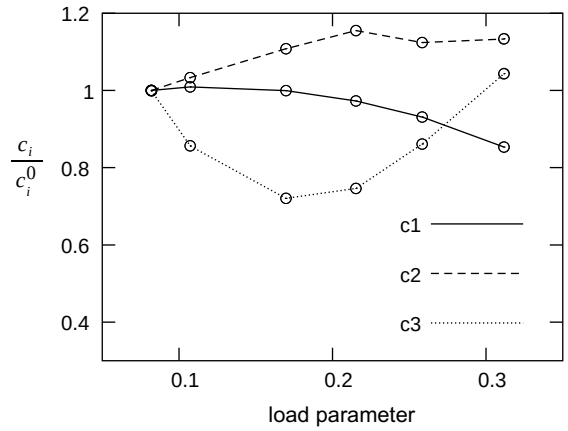

Fig. 12. Normalised principal stiffnesses versus load parameter for a strongly non-proportional loading.

to reach its initial value. This is in contrast to the proportional case where the corresponding stiffness saturates at a significantly smaller value.

5. Discussion

The computed yield surfaces presented in the previous section for the model material considered here suggest a phenomenological representation as a quadratic function in the stresses, i.e. of the form

$$\Omega(\hat{\boldsymbol{\tau}}) = \frac{1}{2}\hat{\boldsymbol{\tau}}\widehat{\mathbb{G}}\hat{\boldsymbol{\tau}}. \tag{81}$$

This has been concluded in similar studies focussing on the initial yield surface of an irregular honeycomb (Chen et al., 1999) and is found here to be a suitable approximation also for finite subsequent deformations. As a refinement, this quadratic function could be augmented to reflect the presence of a bulge at the final stress point of the path that has lead to the respective configuration. The numerical method presented above could be used to produce 'experimental' data in order to find suitable expressions for this refinement. For example, the variation of the direction and magnitude of the inelastic strain rate with the direction of the stress rate can be computed directly.

An important observation is that the elastic and plastic properties of the considered model material are closely related in that the elastic compliance $\widehat{\mathbb{C}}^{-1}$ and the 4th order tensor $\widehat{\mathbb{G}}$ in a quadratic fit of the yield function have practically identical symmetry properties. Further, the above results suggest that both have orthotropic symmetry and that the axes of orthotropy coincide with the principal directions of the plastic stretch $\boldsymbol{U}_{\mathrm{p}}$. It must be noted that this statement refers to the situation where the plastic stretch is measured from an initially isotropic reference configuration as was – at least approximately – the case here. In general, the choice of reference configuration is, of course, arbitrary and the above statement would not make sense without this restriction. It must also be noted that isotropy of the yield and energy function in the virgin state as exhibited in Fig. 3(a) does not imply 'full' isotropy of the material behaviour with respect to the virgin state as the reference configuration. For example, if the microstructure consists of *perfect* honeycombs then yield and energy surfaces are still isotropic, but the hardening is certainly not: *Finite* compression in 1- and 2-direction will lead to a different response because the hexagon has no cubic symmetry (cf. Hohe and Becker, 2003). Random variations of the hexagon-vertex positions have been imposed here also to remove this particular type of anisotropy but it might still be present. In this context, it is not clear if the qualitative difference in the stiffness evolution for the non-proportional and the uniaxial case are a result of this 'initial' anisotropy or of the non-proportionality. Further studies are needed to resolve this question.

A final comment relates to the two dimensional nature of the study. It has already been mentioned that the hydrostatic compression test with a three dimensional beam structure leads to significantly different results in that the pressure exhibits pronounced hardening after the elastic limit. Regarding the conclusions drawn in the preceding paragraph about type and orientation of the evolving anisotropy, the influence of using a two dimensional microstructure is not clear and likewise requires investigation.

Appendix A. The thermodynamic conjugate to $\widehat{\boldsymbol{D}}_{\mathrm{p}}$

With the notations

$$\left(\dot{\boldsymbol{U}}_{\mathrm{p}}\boldsymbol{U}_{\mathrm{p}}^{-1}\right)_{\mathrm{sk}} = \widehat{\boldsymbol{W}}_{0\mathrm{p}} \tag{A.1}$$

the left hand side of (32) reads

$$-J_{\mathrm{p}}\widehat{\boldsymbol{\Sigma}}\cdot\left(\dot{\boldsymbol{U}}_{\mathrm{p}}\boldsymbol{U}_{\mathrm{p}}^{-1}\right) = -J_{\mathrm{p}}\left(\widehat{\boldsymbol{\Sigma}}_{\mathrm{sy}}\cdot\widehat{\boldsymbol{D}}_{\mathrm{p}} + \widehat{\boldsymbol{\Sigma}}_{\mathrm{sk}}\cdot\widehat{\boldsymbol{W}}_{0\mathrm{p}}\right). \tag{A.2}$$

Since $\widehat{\boldsymbol{W}}_{0\mathrm{p}}$ can be calculated from the knowledge of $\widehat{\boldsymbol{D}}_{\mathrm{p}}$ and $\boldsymbol{U}_{\mathrm{p}}$ via (Mehrabadi and Nemat-Nasser, 1987)

$$\widehat{\boldsymbol{W}}_{0\mathrm{p}} = (I_{\boldsymbol{U}_\mathrm{p}} II_{\boldsymbol{U}_\mathrm{p}} - J_\mathrm{p})^{-1}\Big[I^2_{\boldsymbol{U}_\mathrm{p}}(\boldsymbol{U}_\mathrm{p}\widehat{\boldsymbol{D}}_\mathrm{p} - \widehat{\boldsymbol{D}}_\mathrm{p}\boldsymbol{U}_\mathrm{p}) - I_{\boldsymbol{U}_\mathrm{p}}\Big(\boldsymbol{U}^2_\mathrm{p}\widehat{\boldsymbol{D}}_\mathrm{p} - \widehat{\boldsymbol{D}}_\mathrm{p}\boldsymbol{U}^2_\mathrm{p}\Big) + \Big(\boldsymbol{U}^2_\mathrm{p}\widehat{\boldsymbol{D}}_\mathrm{p}\boldsymbol{U}_\mathrm{p} - \boldsymbol{U}_\mathrm{p}\widehat{\boldsymbol{D}}_\mathrm{p}\boldsymbol{U}^2_\mathrm{p}\Big)\Big], \tag{A.3}$$

the second term in (A.2) can be expressed as

$$\begin{aligned}\widehat{\boldsymbol{\Sigma}}_{\mathrm{sk}} \cdot \widehat{\boldsymbol{W}}_{0\mathrm{p}} = \widehat{\boldsymbol{D}}_\mathrm{p} \cdot \Big\{&(I_{\boldsymbol{U}_\mathrm{p}} II_{\boldsymbol{U}_\mathrm{p}} - J_\mathrm{p})^{-1}\Big[I^2_{\boldsymbol{U}_\mathrm{p}}(\boldsymbol{U}_\mathrm{p}\widehat{\boldsymbol{\Sigma}}_{\mathrm{sk}} - \widehat{\boldsymbol{\Sigma}}_{\mathrm{sk}}\boldsymbol{U}_\mathrm{p}) - I_{\boldsymbol{U}_\mathrm{p}}\Big(\boldsymbol{U}^2_\mathrm{p}\widehat{\boldsymbol{\Sigma}}_{\mathrm{sk}} - \widehat{\boldsymbol{\Sigma}}_{\mathrm{sk}}\boldsymbol{U}^2_\mathrm{p}\Big)\\ &+ \Big(\boldsymbol{U}^2_\mathrm{p}\widehat{\boldsymbol{\Sigma}}_{\mathrm{sk}}\boldsymbol{U}_\mathrm{p} - \boldsymbol{U}_\mathrm{p}\widehat{\boldsymbol{\Sigma}}_{\mathrm{sk}}\boldsymbol{U}^2_\mathrm{p}\Big)\Big]\Big\}\end{aligned} \tag{A.4}$$

from which (32) follows with the stress measure $\widehat{\boldsymbol{\Lambda}}$ given explicitly by

$$\begin{aligned}\widehat{\boldsymbol{\Lambda}} = -J_\mathrm{p}\Big\{&\widehat{\boldsymbol{\Sigma}}_{\mathrm{sy}} + (I_{\boldsymbol{U}_\mathrm{p}} II_{\boldsymbol{U}_\mathrm{p}} - J_\mathrm{p})^{-1}\Big[I^2_{\boldsymbol{U}_\mathrm{p}}(\boldsymbol{U}_\mathrm{p}\widehat{\boldsymbol{\Sigma}}_{\mathrm{sk}} - \widehat{\boldsymbol{\Sigma}}_{\mathrm{sk}}\boldsymbol{U}_\mathrm{p}) - I_{\boldsymbol{U}_\mathrm{p}}\Big(\boldsymbol{U}^2_\mathrm{p}\widehat{\boldsymbol{\Sigma}}_{\mathrm{sk}} - \widehat{\boldsymbol{\Sigma}}_{\mathrm{sk}}\boldsymbol{U}^2_\mathrm{p}\Big)\\ &+ \Big(\boldsymbol{U}^2_\mathrm{p}\widehat{\boldsymbol{\Sigma}}_{\mathrm{sk}}\boldsymbol{U}_\mathrm{p} - \boldsymbol{U}_\mathrm{p}\widehat{\boldsymbol{\Sigma}}_{\mathrm{sk}}\boldsymbol{U}^2_\mathrm{p}\Big)\Big]\Big\}.\end{aligned} \tag{A.5}$$

This expression yields the representation (34) for the Cartesian components on the principal axis of $\boldsymbol{U}_\mathrm{p}$. Eqs. (A.3) and (A.5) can also be expressed as

$$\begin{aligned}\widehat{\boldsymbol{W}}_{0\mathrm{p}} &= \widehat{\mathbb{X}}\,\widehat{\boldsymbol{D}}_\mathrm{p},\\ \widehat{\boldsymbol{\Lambda}} &= -J_\mathrm{p}(\widehat{\boldsymbol{\Sigma}}_{\mathrm{sy}} + \widehat{\mathbb{X}}\,\widehat{\boldsymbol{\Sigma}}_{\mathrm{sk}}),\end{aligned} \tag{A.6}$$

involving the 4th order tensor $\widehat{\mathbb{X}}$, whose Cartesian components are given by

$$\widehat{\mathbb{X}}_{ijkl} = (I_{\boldsymbol{U}_\mathrm{p}} II_{\boldsymbol{U}_\mathrm{p}} - J_\mathrm{p})^{-1}\Big[I^2_{\boldsymbol{U}_\mathrm{p}}\Big(U^p_{ik}\delta_{jl} - \delta_{ik}U^p_{jl}\Big) - I_{\boldsymbol{U}_\mathrm{p}}\big(U^p_{in}U^p_{nk}\delta_{jl} - \delta_{ik}U^p_{jn}U^p_{nl}\big) + \Big(U^p_{in}U^p_{nk}U^p_{jl} - U^p_{ik}U^p_{jn}U^p_{nl}\Big)\Big]. \tag{A.7}$$

From (A.7) it is seen that $\widehat{\mathbb{X}}$ has the symmetries

$$\widehat{\mathbb{X}}_{ijkl} = \widehat{\mathbb{X}}_{klij} = -\widehat{\mathbb{X}}_{jilk} \tag{A.8}$$

and therefore yields a skew symmetric 2nd order tensor when operating on a symmetric 2nd order tensor and vice versa.

Appendix B. Derivation of (39)

Eq. (39) is the result of multiplying both sides of (10) by $\boldsymbol{U}^{-\mathrm{T}}_\mathrm{p}$ and $\boldsymbol{U}^{-1}_\mathrm{p}$ from the left and right respectively and using the chain rule. The quantities appearing in (39) are given by

$$\widehat{\mathbb{R}} = \Big[\widehat{\mathbb{C}}\Big(\widehat{\mathbb{K}}^{\mathrm{T}}_{+} + \widehat{\mathbb{K}}^{\mathrm{T}}_{-}\widehat{\mathbb{X}}\Big)\Big]^{-1},$$

$$\text{where } \widehat{\mathbb{K}}_{\pm} = \frac{1}{2}\partial_{\widehat{\boldsymbol{S}}}\Big(\widehat{\boldsymbol{\Sigma}} \pm \widehat{\boldsymbol{\Sigma}}^{\mathrm{T}}\Big),$$

$$\begin{aligned}\text{in Cartesian components } \widehat{\mathbb{K}}_{\pm ijkl} = &\frac{1}{4}\Big(\widehat{C}^e_{ik}\delta_{jl} \pm \delta_{ik}\widehat{C}^e_{jl} + \widehat{C}^e_{il}\delta_{jk} \pm \delta_{il}\widehat{C}^e_{jk}\Big)\\ &+ \frac{1}{2}\widehat{\mathbb{C}}^{-1}_{klpq}\Big(\widehat{S}_{jp}\delta_{iq} \pm \delta_{jp}\widehat{S}_{iq} + \widehat{S}_{jq}\delta_{ip} \pm \delta_{jq}\widehat{S}_{ip}\Big),\end{aligned}$$

$$\text{and } \widehat{\mathscr{A}}_i = \partial^2_{\widehat{\boldsymbol{E}}_\mathrm{e}\widehat{\boldsymbol{M}}_i}\tilde{\psi}_{2\mathrm{e}}. \tag{B.1}$$

Appendix C. Non-orthotropy measure

Employing the matrix notation

$$\begin{bmatrix} \widehat{S}_{11} \\ \widehat{S}_{22} \\ \sqrt{2}\widehat{S}_{12} \end{bmatrix} = \begin{bmatrix} \hat{\mathbb{C}}_{11} & \hat{\mathbb{C}}_{12} & \hat{\mathbb{C}}_{13} \\ \hat{\mathbb{C}}_{12} & \hat{\mathbb{C}}_{22} & \hat{\mathbb{C}}_{23} \\ \hat{\mathbb{C}}_{13} & \hat{\mathbb{C}}_{23} & \hat{\mathbb{C}}_{33} \end{bmatrix} \begin{bmatrix} \widehat{E}_{11} \\ \widehat{E}_{22} \\ \sqrt{2}\widehat{E}_{12} \end{bmatrix} \tag{C.1}$$

for the two dimensional version of Hooke's law (58), i.e.

$$\begin{aligned} &\hat{\mathbb{C}}_{11} = \hat{\mathbb{C}}_{1111}, \quad \hat{\mathbb{C}}_{22} = \hat{\mathbb{C}}_{2222}, \quad \hat{\mathbb{C}}_{33} = 2\hat{\mathbb{C}}_{1212}, \\ &\hat{\mathbb{C}}_{12} = \hat{\mathbb{C}}_{1122}, \quad \hat{\mathbb{C}}_{13} = \sqrt{2}\hat{\mathbb{C}}_{1112}, \quad \hat{\mathbb{C}}_{23} = \sqrt{2}\hat{\mathbb{C}}_{2212}, \end{aligned} \tag{C.2}$$

one can show that ϵ_{ort} is expressible as

$$\epsilon_{\text{ort}} = \min_{\varphi} \sqrt{(\hat{\mathbb{C}}'_{13}(\varphi))^2 + (\hat{\mathbb{C}}'_{23}(\varphi))^2} \Big/ \sqrt{\sum \hat{\mathbb{C}}^2_{ij}}. \tag{C.3}$$

Here, $\hat{\mathbb{C}}'_{ij}(\varphi)$ are the corresponding matrix components of the tensor

$$\widehat{\mathbb{C}}'(\varphi) = \boldsymbol{Q}(\varphi) * \widehat{\mathbb{C}} \tag{C.4}$$

with $\boldsymbol{Q}$ an orthogonal tensor representing a rotation about the x_3-axis. The minimiser φ_{ort} of (C.3) is the direction of the closest orthotropy axes.

References

Akisanya, A.R., Cocks, A.C.F., Fleck, N.A., 1985. The yield behaviour of metal powders. Int. J. Mech. Sci. 39 (12), 1315–1324.

Asaro, R.J., Needleman, A., 1985. Texture development and strain hardening in rate dependent polycrystals. Acta Metall.

Bastawros, A.F., Bart-Smith, H., Evans, A.G., 2000. Experimental analysis of deformation mechanisms in a closed cell aluminum alloy foam. J. Mech. Phys. Solids 48, 301–322.

Bertram, A., 1998. An alternative approach to finite plasticity based on material isomorphisms. Int. J. Plast. 52, 353–374.

Bruhns, O.T., Xiao, H., Meyers, A., 1999. Self-consistent eulerian rate type elastoplasticity models based upon the logarithmic stress rate. Int. J. Plast. 15, 479–520.

Chen, T., Lu, T.J., Fleck, N.A., 1999. Effect of imperfections on the yielding of two dimensional foams. J. Mech. Phys. Solids 47 (11), 2235–2272.

Cleja-Tigoiu, 2003. Consequences of the dissipative restrictions in finite anisotropic elasto-plasticity. Int. J. Plast. 19, 1917–1964.

Coleman, B.D., Gurtin, M.E., 1967. Thermodynamics with internal state variables. J. Chem. Phys. 47 (2), 597–613.

Dafalias, Y.F., 1998. Plastic spin: necessity or redundancy. Int. J. Plast. 14 (9), 909–931.

Deshpande, V., Fleck, N.A., 1999. Multi-axial yield of aluminium alloy foams. In: Banhart, J., Ashby, M.F., Fleck, N.A. (Eds.), Metal Foams and Porous Metal Structures. MIT Publishing, pp. 247–254.

Eidel, B., Gruttmann, F., 2003. Elastoplastic orthotropy at finite strains: multiplicative formulation and numerical implementation. Comput. Mater. Sci.

Ekh, M., Runesson, K., 2001. Modeling and numerical issues in hyperelasto-plasticity with anisotropy. Int. J. Solids Struct. 38, 9461–9478.

Gibson, L.J., Ashby, M.F., 1998. Cellular Solids. Pergamon Press.

Hackl, K., 1997. Generalized standard media and variational principles in classical and finite strain elastoplasticity. J. Mech. Phys. Solids 45 (5), 667–688.

Halphen, B., Nguyen, Q.S., 1975. Sur les materiaux standards generalises. J. Mech. 14, 39–63.

Hill, R., 1948. A variational principle of maximum plastic work in classical plasticity. Quart. J. Mech. Appl. Math. 1, 18–28.

Hill, R., 1967. The essential structure of constitutive laws for metal composites and polycrystals. J. Mech. Phys. Solids 15, 79–95.

Hill, R., 1978. Aspects of invariance in solid mechanics. In: Yih, C.S. (Ed.), Advances in Applied Mechanics, vol. 18. Academic Press.

Hill, R., Rice, J.R., 1973. Elastic potentials and the structure of inelastic constitutive laws. SIAM J. Appl. Math. 25 (3), 448–461.

Hohe, J., Becker, W., 2003. Effective mechanical behaviour of hyperelastic honeycombs and two dimensional model foams at finite strain. Int. J. Mech. Sci. 45, 891–913.

Kocks, U.F., Tomé, C.N., Wenk, H.-R., 1998. Texture and Anisotropy. Cambridge University Press.

Löblein, J., Schröder, J., Gruttmann, F., 2003. Application of generalized measures to an orthotropic finite elasto-plasticity model. Comput. Mater. Sci. 28, 696–703.

Lubarda, V.A., Krajcinovic, D., 1995. Some fundamental issues in rate theory of damage-elastoplasticity. Int. J. Plast.

Lubliner, J., 1986. Normality rules in large defromation plasticity. Mech. Mater. 5, 29–34.

Mandel, J., 1974. Thermodynamics and plasticity. In: Delgado, J.J., Nina, N.R., Whitelaw, J.H. (Eds.), Foundations of Continuum Thermodynamics. Mcmillan, London, pp. 283–304.

Maugin, G.A., 1994. Eshelby stress in elastoplasticity and ductile fracture. Int. J. Plast. 10, 393–408.

Mehrabadi, M.M., Nemat-Nasser, S., 1987. Some basic kinematical relations for finite deformation of continua. Mech. Mater. 6, 127–138.

Menzel, A., Steinmann, P., 2003. Geometrically non-linear anisotropic inelasticity based on fictitious configurations: application to the coupling of continuum damage and multiplicative elasto-plasticity. Int. J. Numer. Methods Eng. 56 (14), 2233–2266.

Miehe, C., 1998. A constitutive frame of elastoplasticity at large strains based on the notion of a plastic metric. Int. J. Solids Struct. 35 (30), 3859–3897.

Miehe, C., Apel, N., Lambrecht, M., 2002. Anisotropic additive plasticity in the logarithmic strain space: modular kinematic formulation and implementation based on incremental minimization principles for standard materials. Comput. Methods Appl. Mech. Eng. 191, 5383–5425.

Papadopoulos, P., Lu, J., 2001. On the formulation and numerical solution of problems in anisotropic finite plasticity. Comput. Methods Appl. Mech. Eng. 190, 4889–4910.

Reese, S., 2003. Anisotropic elastoplastic material behaviour in fabric structures. In: Miehe, C. (Ed.), Computational Mechanics of Solid Materials at Large Strains, IUTAM Symposium, pp. 201–210.

Rice, J.R., 1971. Inelastic constitutive relations for solids: an internal variable theory and its application to metal plasticity. J. Mech. Phys. Solids 19, 433–455.

Rice, J.R., 1975. Continuum mechanics and thermodynamics of plasticity in relation to microscale deformation mechanisms. In: Argon, S. (Ed.), Constitutive Equations in Plasticity. M.I.T. Press, Cambridge Mass, pp. 23–79 (Chapter 2).

Rottmann, G., Coube, O., Riedel, H., 2001. Comparison between triaxial results and model predictions with special consideration of the anisotropy. In: Proceedings of the European Congress on Powder Metallurgy 2001, vol. 3. EPMA, pp. 29–37.

Rubin, M.B., 1994. Plasticity theory formulated in terms of physically based microstructural variables – Part I. Theory. Int. J. Solids Struct. 31 (19), 2615–2634.

Scheidler, M., Wright, T.W., 2001. A continuum framework for finite viscoplasticity. Int. J. Plast. 17, 1033–1085.

Schmidt, I. Some comments on formulations of anisotropic plasticity. Comput. Mater. Sci., in press.

Sidoroff, F., Dogui, A., 2001. Some issues about anisotropic elastic–plastic materials at finite strain. Int. J. Solids Struct. 38, 9569–9578.

Svendsen, B., 2001. On the modelling of anisotropic elastic and inelastic material behaviour at large deformation. Int. J. Solids Struct. 38, 9579–9599.

Tsakmakis, C.h., 2004. Description of plastic anisotropy effects at large deformations – Part I. Restrictions imposed by the second law and the postulate of Il'iushin. Int. J. Plast. 20, 167–198.

Ziegler, H., Wehrli, C., 1987. The derivation of constitutive relations from the free energy and the dissipation function. In: Wu, Th.Y., Hutchinson, J.W. (Eds.), Advances in Applied Mechanics, vol. 25. Academic Press.